SYNTHESIS AND OPTIMIZATION OF CARBON NANOFIBER TEMPLATED POLYPYRROLE

by

AYÇA ERDEN

Submitted to the Graduate School of Engineering and Natural Sciences
in partial fulfillment of
the requirements for the degree of
Master of Science

Sabancı University
Fall 2008

© Ayça Erden 2008

All Rights Reserved

SYNTHESIS AND OPTIMIZATION
OF
CARBON NANOFIBER TEMPLATED POLYPYRROLE

Ayça Erden

Material Science and Engineering, MS Thesis, 2007

Thesis Supervisor: Prof. Dr. Yuda Yürüm

Keywords: Supercapacitor, Pyrrol, Polypyrrol, Carbon Nanofiber, Conducting Polymer

ABSTRACT

In order to suggest a new promising material to be used as an active material in supercapacitor applications, carbon nanofiber templated Polypyrrole was designed and synthesized.

The common conducting polymer/ carbon nanofiber composites used in capacitive applications were usually physically mixed composites of the materials. In this thesis, the outcomes are investigated when these materials of interest are chemically bonded via electropolymerization.

Carbon nanofibers with a thickness of 100 nm to 150 nm were chosen to act as a template for the conducting polymer to grow on. The electropolymerization was successful and it is proven by voltammetric measurement, Nuclear Magnetic Resonance spectra, Fourier Transform Infrared spectra and Scanning Electron Microscopy images.

After the deposition of Polypyrrole on carbon nanofibers were achieved, the material was optimized by means of the deposition amount and speed. The results were supported by voltammograms, specific capacitance calculations and SEM images.

Polymers with different deposition amounts and speeds are compared. The sample deposited by six times cycling at 25 mV/s is found to posses both the highest specific capacitance and the highest surface area.

KARBON NANOFİBER ŞABLONLU POLİPİROLÜN SENTEZİ VE OPTİMİZASYONU

Ayça Erden

Malzeme Bilimi ve Mühendisliği, Yüksek Lisans Tezi, 2007

Tez Danışmanı: Prof. Dr. Yuda Yürüm

Anahtar Kelimeler: Süperkapasitör, Pirol, Polipirol, Karbon Nanofiber, İletken Polimer

ÖZET

Süperkapasitör uygulamalarında kullanılması amaçlanan yeni ve gelecek vaat eden bir malzeme, karbon nanofiber şablonlu Polipirol tasarlanmış ve sentezlenmiştir.

Yük depolama araçlarında genel olarak kullanılan iletken polimer/ karbon nanofiber kompsiteleri fisiksel olarak elde edilir. Bu çalışmada, bahsedilen malzemelerin elektrokimyasal olarak polimerleştirilme sonucu kimyasal yolla bağlanmiş kompositlerinin özellikleri incelenmiştir.

Polimerin üzerinde sentezleneceği şablon olarak seçilen karbon nanofiberlerin kalınlıkları 100 nm ile 150 nm arasında değişmektedir. Electropolimerleşme başarılı olmuş ve sonuçları voltammetrik ölçümlerle, Nükleer Manyetic Rezonans spektra, Fourier Transform Kızılötesi spektra ve Taramalı Elektron Mikroskopisi görüntüleri ile desteklenmiştir.

Karbon nanofiberler üzerinde pirolün polimerleştirilmesi başarıyla gerçekleştirildikten sonra, malzeme kaplama miktarı ve kaplama hızı kriterlerine göre optimize edilmiştir. Sonuçlar were supported by voltamogramlar, spesifik kapacitans hesaplamaları ve SEM görüntüleri ile desteklenmiştir.

Farklı miktarda olan var farklı hızlarda polipirol karşılaştırılmış, 25 mV/s tarama hızında 6 dönüşle kaplanmış olan polipirol örneğinin en yüksek spesifik kapasitans ve yüzey alani özelliklerini gösterdiği görülmüştür.

TO MY BELOVED MENTOR
GÜRSEL SÖNMEZ
AND
TO MY FAMILY
WITH FULL COMPLIMENTS

ACKNOWLEDGEMENTS

I would like to express my greatest appreciations to Prof. Dr. Yuda Yürüm and Assoc. Prof. Yusuf Ziya Menceloğlu for their guidance and encouragements throughout this work.

I especially thank to Prof. Dr. Levent Toppare for never leaving side of me, for his endless help, and for his sightful guidence.

Special thanks to Dr. Hayal Bülbül Sönmez for helping me dealing with the obsticles I have faced.

I would like to thank especially to MSc. Evren Aslan Gürel and MSc. Deniz Yılmaz for their support, help, patience and friendship. They were with me whenever I needed, no matter how much distance there was between us.

Also, I want to thank to my best friends Handan Doğan and Ceyda Yazıcı for their support and confidence in me. With them, I was never alone even at the hardest times throughout this work.

Appreciation is extended to colleagues in Material Science and Engineering Program, Sabanci University.

I would like to thank to my family for always being there for me.

Finally I thank to Gürsel Sönmez; for being a friend as well as a wonderful guide in the little time I had known him as my advisor. I hereby dedicate this work in memory of him. I will remember him and the things he thought me as long as I live.

TABLE OF CONTENTS

CHAPTER 1 1
INTRODUCTION 1
1. 1. Conducting Polymers 1
1. 1. 1. Basic Principles 1
1. 1. 2. Electrical Conductivity in Conducting Polymers 3
1. 1. 2. 1. Band Theory 3
1. 1. 2. 2. Doping Process 4
1. 1. 2. 3. Charge Carriers in Conducting Polymers 5
1. 1. 2. 4. Hopping Mechanism 6
1. 1. 3. Electropolimerization 7
1. 1. 4. Applications of Conducting Polymers 9
1. 2. Carbon Nanofibers 10
1. 3. Supercapacitors 12
1. 3. 1. Energy Storage Mechanism of Supercapacitors 12
1. 3. 2. Conducting Polymers and Carbon Nanotubes for Supercapacitor Applications 14
1. 4. Aim of the Study 15
CHAPTER 2 16
EXPERIMENTAL 16
2.1. Materials 16
2.2. Instrumentation 16
2.2.1 Potentiostat 16
2.2.2. Electrolysis Cell 17
2.2.4. BET 17
2.2.5. Solid State NMR 18
2.2.6. FTIR 18
2.3. Procedure 19
2.3.1. Synthesis of Carbon Nanofibers* 19
2.3.1.1. Catalyst preparation 19
2.3.1.2. Carbon nanofiber and nanotube production 20
2.3.1.2. a. Optimization of the growth conditions 20
2.3.1.2. b. Kinetic Studies 22
2.3.2. Deposition of Polypyrrole on Carbon Nanofibers 23
2.3.2.1. Preparation of the Working Electrode 23
2.3.2.2. Deposition 23
CHAPTER 3 24
RESULTS and DISCUSSION 24
3.1. Optimization 24
3.1.1. Optimization of the Number of Cycling 24
3.1.2. Optimization of the Scan Rate 33
3. 2. 1. NMR 43
3. 2. 1. a. C^{13} NMR Spectroscopy 43
3. 2. 1. a. N^{15} NMR Spectroscopy 43
3. 2. 3. a. Scan Rate Dependence 48
CHAPTER 4 50
CONCLUSION 50
REFERENCES 51

LIST OF TABLES AND FIGURES

Figure 1.1 Some common conducting polymers 3

Figure 1.2 Schematic representation of band structure of metal, semiconductor and insulator. (Dark regions represent the valence band and white regions stand for conduction band) 4

Figure 1.4 Formation of polarons and bipolarons on Polypyrrole 6

Figure 1.5 Electrochemical polymerization mechanism. 8

Table 1.1 A summarization of the progress since the discovery of CNF's by means of applications. 11

Figure 1.6 Schematic representation of an supercapacitor: + signs are cations of the electrolyte and – signs are anions of the electrolyte. 13

Figure 2.1 Production scheme of the catalysts.....20

Figure 2.2 CVD process set-up for carbon nanostructure production.....21

Figure 2.3 A schematic representation of the electrolysis cell.....23

Figure 3.1 SEM images of uncoated CNF's used as a template for PPy 25

Figure 3.2 The voltammograms of a) Polypyrrole on ITO, b) baseline of the CNF/Cu plate/ITO electrode, and c) monomer oxidation of Polypyrrole on CNF. 26

Figure 3.3 Monomer oxidation voltammogram of CNF templated PPy. 27

Figure 3.4. Two voltammograms of CNF templated PPy with different amounts of deposition and their consequent SEM images: (a) 5 times cycled (b) 10 times cycled. 28

Figure 3.5 Voltammogram and SEM image of CNF templated PPy via 6 times cycling 29

Figure 3.6 Voltammogram and SEM image of CNF templated PPy via 7 times cycling at 100 mV/s scan rate. 30

Figure 3.7 Voltammogram and SEM image of CNF templated PPy via 7 times cycling at 100 mV/s scan rate. 31

Figure 3.8 Voltammogram and SEM image of CNF templated PPy via 7 times cycling at 100 mV/s scan rate. 32

Figure 3.9 The voltammogram of CNF templated PPy deposited via 6 times cycling at a scan rate of 25 mV/s, and its SEM images: (b) 20000 times magnified (c) 50000 times magnified. 34

Figure 3.10 SEM images of 6 times cycled CNF Templated PPy (at 25 mV/s scan rate): (a) 50000 times magnified (b) 100000 times magnified. 35

Figure 3.11 The voltammogram of CNF templated PPy deposited via 6 times cycling at a scan rate of 50 mV/s, and its SEM images: (b) 20000 times magnified (c) 50000 times magnified. 37

Figure 3.12 The voltammogram of CNF templated PPy deposited via 6 times cycling at a scan rate of 75 mV/s, and its SEM images: (b) 20000 times magnified (c) 50000 times 38

Figure 3.13 The voltammogram of CNF templated PPy deposited via 7 times cycling at a scan rate of 150 mV/s, and its SEM images: (b) 20000 times magnified (c) 50000 times magnified. 40

Figure 3.14 The voltammogram of CNF templated PPy deposited via 6 times cycling at a scan rate of 200 mV/s, and its SEM images: (b) 20000 times magnified (c) 50000 times magnified. 41

Figure 3.15 The SEM image of CNF templated PPy deposited via 6 times cycling at a scan rate of 200 mV/s, 50000 times magnified. 42

Figure 3.16 NMR shifts of (a) Pyrrolidine, (b) Pyrrole 43

Figure 3.17 C13 NMR of CNF templated PPy deposited via 6 times cycling at 25 mV/s scan rate. 44

Figure 3.18 N^{15} NMR of CNF templated PPy deposited via 6 times cycling at 25 mV/s scan rate.....45

Figure 3.20 Scan rate dependence voltammograms of PPy (a) on ITO (b) on CNF.....48

LIST OF ABBREVIATIONS AND SYMBOLS

ABBREVIATIONS

MeCN ..... Acetonitrile
CB..... Conductance band
HOMO..... Highest occupied molecular orbital
LUMO..... Lowest unoccupied molecular orbital
PA..... Polyacetylene
PPy..... Polypyrrole
Py..... .Pyrrole
VB..... Valence band
ESR ..... Equivalent Series Resistant
ITO..... Indiun Tin Oxide Coated Glass Slide
CNT..... Carbon Nanotube
CNF..... Carbon Nanofiber
CP..... Conducting Polymer
SWNT..... Single-walled Nanotube
MWNT..... Multi-walled Nanotube
PECVD..... Plasma-Enhanced Chemical Vapor Deposition

GREEK

α.....1− position of the heterocycle
β.....2− position of the heterocycle
π.....pi-bonding orbital
π□.....pi-antibonding orbital
ε.....Permittivity/ Dielectric Constant

CHAPTER 1

INTRODUCTION

1. 1. Conducting Polymers

1. 1. 1. Basic Principles

Until about 30 years ago all carbon based polymers were rigidly regarded as insulators. Conducting polymers (CPs) are organic materials possessing electrical, electronic, magnetic and optical properties of a metal while retaining the mechanical properties and processability to a certain extent.

It has been known for more than 40 years that the electric conductivity of the conjugated polymer chains is by orders of magnitude higher than that of other polymeric materials now. Traditionally polymers were thought of as insulators and any

electrical conduction in polymers was generally regarded as an undesirable phenomenon until in the 1970s somewhat surprisingly a new class of polymers possessing high electronic conductivity (electronically conducting polymers) in partially oxidized (or less frequently reduced) state has been discovered[1]. Pohl, Katon and others first synthesized and characterized semiconducting and conjugated polymers in 1960's[2,3]. The discovery of poly(sulphur nitride) [$(SN)_x$] in 1975, which becomes superconducting at low temperatures[4], a polymeric inorganic explosive and its interesting electrical properties[5,6] were a step towards conducting polymers as they are known today. This discovery of conducting polymers was unique in its accomplishment as a possible substitute for metallic conductors and semi-conductors due to their ability to be changed by means of electrical, mechanical, optical and thermal properties due to tailoring[7].

Conducting polymer research was accelerated when Shirikawa and coworkers[8] discovered in 1974 that the electronic conductance of polyacetylene (PA) maybe further increased by many orders of magnitude by "doping it" with electron acceptors (p-type dopants) such as iodine[9]. The term "conducting polymers" was coined after the American scientists Heeger and MacDiarmid, whose work was triggered the rapid growth of research in this field, discovered that the polyacetylene, $(CH)_x$, synthesized via the method of Shirakawa and colleagues, could become highly conducting on exposure to oxidizing or reducing agents in 1977[10,11]. The successful doping of PA -in electrochemical terminology the equivalent of oxidation or reduction- encouraged the same scientists to test PA as a rechargeable active battery electrode[12]. They were able to enhance the electrical conductivity of PA (10^{-9} Scm^{-1}) by several orders by doping with oxidizing agents e.g. I_2 and AsF_5. This discovery could be considered as the starting point of the modern area of conducting polymers[13].

Polyacetylene was initially the most studied CP from both scientific and practical applications of point of view. However, due to its high chemical instability in air and related factors, interest in it has been recently confined to its scientific aspect.

Polypyrrole (PPy) has been investigated the most among polyheterocyclics. The electrochemical oxidation of pyrrole can be carried out on platinum electrode. The product is a conducting polymer known as 'Pyrrole Black' produced coherent films of

PPy with a conductivity of 100 Scm^{-1} and exhibited excellent air stability. However, the main hindrance of its processability is in its insolubility in any organic solvents[14].

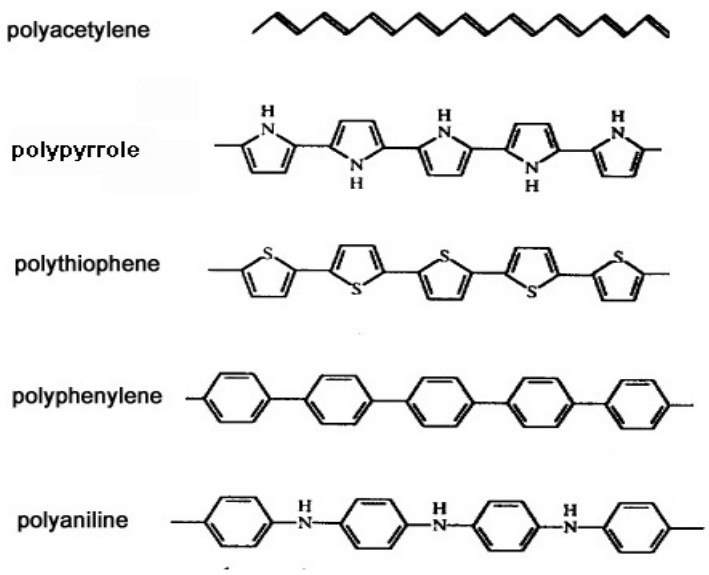

Figure 1.1 Some common conducting polymers

In the course of these studies conducting polymers with similar to PA were discovered or rediscovered, such as polyparaphenylene, polypyrrole, polythiophene and, last but least, polyaniline (Figure 1.1). However, it soon become apparent that the pathway from inspiration to practical realization can be long and thorny, that much basic research on a broad, interdisciplinary basis still has to be done[15].

1. 1. 2. Electrical Conductivity in Conducting Polymers

1. 1. 2. 1. Band Theory

According to their ability to conduct electricity, materials are classified as metals, semiconductors or insulators. Electrical conductivity is directly proportional with number density of mobile charge carriers (n), the carrier charge (q), and the carrier mobility (μ), and given by the following formula:

$$\sigma = q\ n\ \mu$$

The kind of mechanism a material follows to conduct electricity is explained by band theory. The overlapping valence electrons produce a valence band; meanwhile the electronic levels above them remaining empty are to produce the conduction band. The energy difference between two levels is called band gap, which the valence electrons should bear the sufficient energy to overcome. In metals, the valence shell is partially occupied resulting in zero band gap, therefore electrons can freely flow to the conduction band[16]. Where as in semiconductors, the valence electrons may need to be excited to the conduction band by means of thermal excitation, vibrational excitation or excitation by photons. Existence of too large band gap will lead to some difficulties of promotion of electrons from the valence band to the conduction band. Compounds of such property are referred as insulators. Band structure of a metal, a semiconductor and an insulator are shown in Figure 1.2.

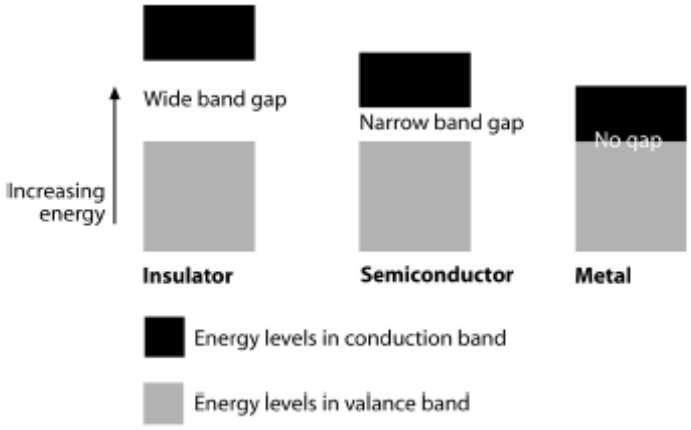

Figure 1.2 Schematic representation of band structure of metal, semiconductor and insulator. (Dark regions represent the valence band and white regions stand for conduction band)

1. 1. 2. 2. Doping Process

The term "doping" corresponds to a redox reaction in electrochemical terminology; therefore it can be classified as "p-doping" and "n-doping" meaning polymer oxidation by anions and reduction by cations respectively. The associated anions/ cations are called as dopants.

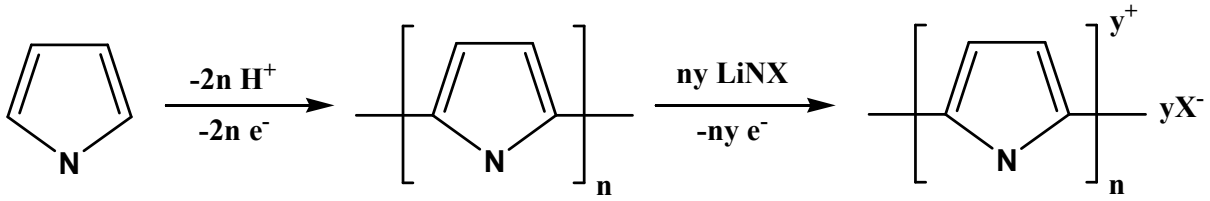

Figure 1.3 Doping figure of anodic oxidative polymerization of pyrrole.

Doping a polymer by donor/ acceptor radicals or with oxidative/reductive substitutents results in increasing the conductivity several-fold[17]. Doping of conductive polymer involves random dispersion or aggregation of dopants in molar concentrations in the disordered structure of, polarons and bipolaron in the polymer chain[18]. The extent of oxidation/reduction is called doping level, which is generally measured as the proportion of dopant ions or molecules incorporated per monomer unit. Increased doping level leads to higher conductivity by the creation of more mobile charges.

1. 1. 2. 3. Charge Carriers in Conducting Polymers

Neutral state of conducting polymers is somewhat poor in the means of conductivity. However; a drastic increase in conductivity reveals as soon as charge carriers are introduced in between the valence band and the conduction band.

When polymers are doped the conjugated backbone is delocalized, and the resulting overlapping π-orbitals are continuous. Therefore a new degeneracy is produced in the frontier molecular orbitals. The occupied (The Highest Occupied Molecular Orbital- HOMO) and the unoccupied (The Lowest Unoccupied Molecular Orbital- LUMO) are built making the conducting polymers classified as semi-conductors.

Degeneracy in the backbone of polyacetylane, which is the simplest conducting polymer, is the origin of structural defects resulting in bond alteration. A single unpaired electron exists at the defect position, although the overall charge remains zero, creating a new energy level at mid-gap called a soliton. Oxidation of the polymer breaks one double bond leaving a radical and a positive charge on the polymer chain, which is referred as polaron[19]. As the doping process continues, polarons unite to form bipolarons. The combination of these two radicals generates a new Π bond, which is more stable than two polarons at the same distance apart. Upon increasing oxidation level, the polarons get closer to each other to form Π bonds and the remaining positive

charges achieve high mobility along the chain[20]. At this point, remarkable increase is observed in the conductivity.

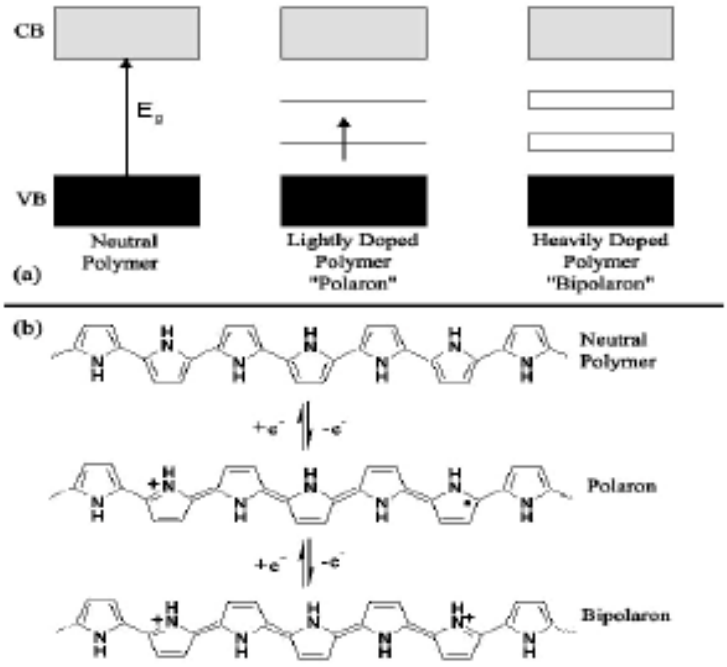

Figure 1.4 Formation of polarons and bipolarons on Polypyrrole

In order to have place for charge dismissal in the HOMO and for insertion in the LUMO, charge is localized in the non-bonding molecular orbitals in the doped polymer. Since the delocalized backbone provides the possibility for the soliton to take place anywhere on the chain, mobility is granted and therefore electronic conductivity has a suggested mechanism.

1. 1. 2. 4. Hopping Mechanism

Many structural imperfections exist in CP's and electrical conductivity depends on these structural defects as well as the charge carriers that are discussed afore. Therefore in the means of bulk conductivity, these defects are needed to be taken into account. Conductivity is not only a result of charge transfer along the chain, but is also due to electron hopping between chains and between different conjugated segments of the same chain[21]. In addition to these effects, which act at a molecular level, bulk

conductivity values are also dominated by electron transfer between grain boundaries and variation in morphology[22,23].

1. 1. 3. Electropolimerization

Electrochemical polymerization is run in a preferred solvent containing an ionic dopant salt with the monomer of interest dissolved in. By application of anionic potential, the monomer is oxidized on the surface of the electrode named working electrode. Choosing the right solvent and the electrolyte is crucially important in electrochemical polymerization since while providing a conductive environment, they should not exhibit any instability in-between the potential interval of the monomer[23].

The suitable solvent should have very large potential windows, and high relative permittivities, which allow a good dissociation of the electrolyte and thus a good ionic conductivity like the organic solvents such as acetonitrile (ACN) and propylene carbonate (PC).

Plenty of mechanisms are proposed for the electropolimerization process up to now since the mechanism phenomena is debatable. The rapidness of the reaction has been the primary obstacle in determining of the reaction steps. Another difficulty faced during researches are in the characterization and the analysis of physical properties since, besides their amorphous nature, almost all CP's are insoluble until the recent examples[24, 25,26, 27, 28]. Altough, there has not been a solid agreement among researchers concerning this mechanism issue because of the problems listed above, the mechanism suggested by Diaz et al.[29] is the most often preferred in the literature. This mechanism was verified by Waltman and Bargon[30] based on the theoretical studies on the radical cations with high reactivity of the unpaired electron density. It is initiated by electron transfer (E) followed by a series of chemical reactions ("C) and electron transfer reactions. The term ECE, which is a short term for E(CE)n, is often used to describe all the reactions involved in the formation of the film by electropolymerization. This mechanism can be illustrated as shown in Figure 1.5 and the pathway is as the following:

i. Oxidation of the monomer to a radical cation by loss of electron from the monomer. The oxidation of this radical cation is usually irreversible which shows

that the cation radical formed in the first step is extremely reactive.

ii. Coupling of two radicals to produce a dihydro dimer dication and rearomatization, which constitutes the driving force of the chemical step.

iii. Proton loss occurs to yield a neutral dimer and rearomatization.

iv. Oxidation of the dimer to its radical cation. Due to the applied potential, the dimer, which is more easily oxidized than the monomer, occurs in its radical form.

v. Reaction of the dimer radical cation with another radical cation.

vi. Electrochemical polymerization proceeds then through successive electrochemical and chemical steps until the oligomer becomes insoluble in the electrolytic medium and precipitates onto the electrode surface. The electrochemically prepared polymer film is already doped and contains the counterion.

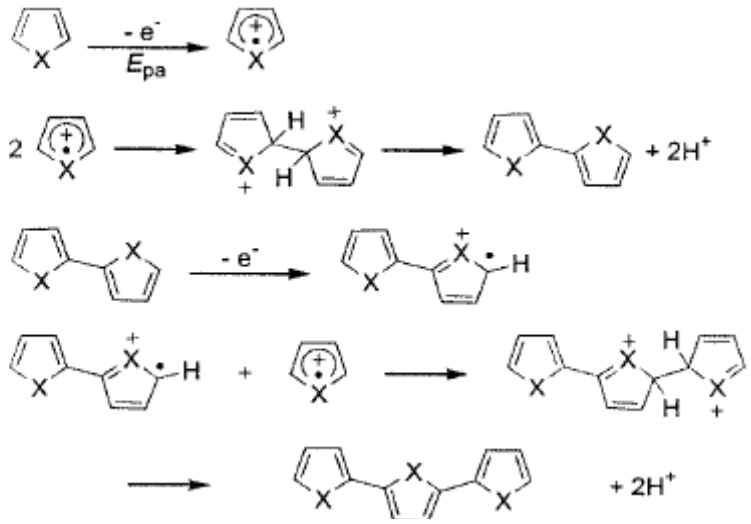

Figure 1.5 Electrochemical polymerization mechanism.

As explained above, the initial oxidation results in the radical cation of the monomer which reacts with other monomers present in the solution to form oligomeric products and then the polymer. The extended conjugation in the polymer results in a lowering of the oxidation potential compared to the monomer. Therefore, the synthesis and doping of the polymer are generally done simultaneously. The anion is incorporated into the polymer to ensure the electrical neutrality of the film and, at the end of the reaction; polymeric film of controllable thickness is formed at the anode. The anode can be made of a variety of materials including platinum, gold, glassy carbon, and tin or indium-tin

oxide (ITO) coated glass. The electropolymerization is generally achieved by potentiostaic (constant potential) or galvanostatic (constant current) methods.

1. 1. 4. Applications of Conducting Polymers

Conducting polymers have a great promise for very wide range of usage areas: Sensors, batteries, electrochromic displays, diodes and transistors, supercapacitor, etc. This interest is largely due to the wide range of possible applications because of their ease of synthesis, ease of tailoring and processability, good environmental stability and long term stability of electrical conductivity. What specific use the conducting polymer film would be assigned is mostly determined by the porosity of the conducting polymer film.

Another electrochemical application of conducting polymers may be their use as electrochromic displays (ECD)[31,32,33,34]. ECD's are based on the fact that the color of a polymer changes during electrochemical charging and discharging. Thus, polyaniline appears, to be particularly promising, as its colors changes during oxidation from yellow, through green, to blue and violet, and this process is reversed during discharging. Polythiophenes are especially convenient for display purposes because they show color change from red to blue on applying voltage. The changed color lasts for several hours, thus showing the possibility of being used as an optical memory element. Moreover, polythiophene can also be conveniently used as the switching element because the switching time from red to blue is 80 msec. Lately, there are promising research findings on the color "green" which completes the RGB (red-green-blue) color scheme to construct the full color scale.[35,36,37,38] The electrochromic properties of conducting polymers can be exploited to produce thermal smart windows as well as displays. The smart windows absorb some of sunlight, which changes color in response to sunlight or temperature changes, thus saving air conditioning cost.

The high ability of recycling of conductive polymers makes them suitable candidates as cathodes in rechargeable batteries. Using conducting polymers in this aspect brings many advantages to the process such as ease of fabrication, processability, low cost and light weight. The first polyacetylene-lithium battery was published in

1981[39]. Conductive polymer batteries have long life, are rechargeable and can produce high current density. For polypyrrole[40] and polyaniline[41] commercially available cells already exist or are in preparation.

1. 2. Carbon Nanofibers

Carbon nanofibers (CNF) were discovered in 1991 as a minor byproduct of fullerene synthesis[42]. Remarkable progress has been made in the ensuring 14 years, ,including the discovery of two basic types of nanotubes (single-wall and multiwall); great strides have been taken in their synthesis and purification, elucidation of the fundamental physical properties, and important steps are being taken toward realistic practical applications[43, 44,45].

Carbon nanotubes' morphology is considered equivalent to a graphene sheet rolled into a seamless tube capped on both ends whereas; CNF's are basicly long cylinders of 3-coordinated carbon, slightly pyramidalized by curvature[46] from the pure sp2 hybridization of graphene, toward the diamond-like sp3. Infinitely long in principle, a perfect tube is capped at both ends by hemi-fullerenes, leaving no dangling bonds. A single-walled carbon nanotube (SWNT) is one such cylinder, while multiwall tubes (MWNT) consist of many nested cylinders whose successive radii differ by roughly the interlayer spacing of graphite[47,48]. Nanotubes are distinguished from less-perfect quasi-one-dimensional carbon materials by their well- developed parallel wall structure. The unique feature of carbon nanotubes is that they exist in both metallic and semiconducting varieties. This phenomenon depends on the atomic arrangement of the carbon atoms making up the nanotube (chirallity), and makes it possible to create nanoelectronic devices, circuits, and computers using SWNT's.

There have been tremendous advance in nanofiber and nanotube synthesis since 1991. Synthesis methods have been seen to occur in a wide range of environments. Whether near the focus of a high-powered laser[49], in between two arching graphite electrodes[50], in a hot furnace full of hydrocarbon gas[51], or even in the middle of a flame[52], nanotubes form given the right conditions. The basic perquisites for the formation of CNT's are an active catalyst, a source of carbon, and adequate energy. The

common synthesis methods can be listed as: Arc discharge synthesis, laser ablation synthesis, thermal synthesis, and plasma-enhanced chemical vapor deposition (PECVD) synthesis. Some of the obstacles preventing CNT's from commercial usage, such as yield, purity, and alignment, have recently been satisfactorily overcomed. Nevertheless, there still remain challenges for chirality and diameter control. For many applications, such as chemical and biological sensors, the current level of control may be nearly sufficient for commercial deployment. Yet, in order to realize the more ambitious goals of nanofiber-based electronics using nanofiber FETs and nanofiber interconnects, to take full advantage of the remarkable properties of nanofiber, more work remains to be done by means of synthesis research[53].

Materials	Devices
Chemical and biological separation, purification and catalysis.	Probes, sensors, and actuators for molecular imaging, sensing, and manipulation.
Energy storage such as hydrogen storage, fuel cells and the lithium battery.	Transistors, memories, logic devices, and nanoelectronic devices.
Composites for coating, filling, and structural materials.	Field emission devices for x-ray instruments, flat panel displays, and other vacuum nanoelectronic applications.

Table 1.1 A summarization of the progress since the discovery of CNF's by means of applications.

The exponential growth of the portable electronic devices' market together with the development of electric vehicles has created a continuously increasing demand for lightweight and compact electric power sources of high energy and power density. For many years, nanotextured carbons have been shown as a basic material for the realization of high-performance power-sources, e.g., supercapacitors, lithium-ion accumulators, or fuelcells. The key factors that dictate the selection of carbon for this target are its accessibility, low cost, easy processability, as well as the different forms attainable (powder, fibers, foams, fabrics, composites)[54], adaptable porosity[55,56], and surface functionality[57,58]. A wide variety of carbon materials, e.g., graphites, cokes, activated carbons, aerogels, carbon blacks, carbon nanotubes, etc. have been extensively

considered as electrode materials for energy storage because of the amphoteric character of carbons, in other words, being both electron donor and acceptor[59].

Composite materials reinforced with carbon or graphite fibers are often used in sporting-goods, high-performance aircraft, and other applications where high stiffness and lightweight are required. Vapor-grown carbon fibers, used as conductivity additives for paints and plastics, are sold commercially for quite some time. CNF's have received a good deal of attention lately as catalyst supports, fuel cells, and battery electrodes[60].

1. 3. Supercapacitors

Electrical energy can be stored in two fundamental ways:

i. indirectly in batteries as potentially available chemical energy requiring Faradaic oxidation and reduction of the electrochemically active reagents to release charges that can perform electrical work when they flow in-between two electrodes having different potentials.

ii. directly, in an electrostatic way, as negative and positive electric charges on the plates of a capacitor, a process known as non-Faradaic electrical energy storage.

1. 3. 1. Energy Storage Mechanism of Supercapacitors

Supercapacitors (often called electrochemical capacitors or ultracapacitors)[61,62,63] are devices that store electrical energy on the basis of the phenomena that interfacial capacity is increased as the surface area of electrode of interest. They have been aroused interest for various applications including portable systems and automotive applications due to their high specific power and very long durability. In most cases, being often associated to a battery, they are used to deliver a high power during a short time, which in turn provides a high specific energy. Some applications of supercapacitors are hybrid power sources for electrical vehicles, computers, UPS, pulse laser technique, starters for engines, etc.

In a true electrochemical capacitor the charges are accumulated in the electrical double layer at the electrode/electrolyte interface. In contrast with typical accumulators, this process occurs without any charge transfer (faradaic) reaction. An electrochemical capacitor is constituted of two electrodes on which the ions are fixed, the positive one with electron deficiency and the second one with electron excess. The capacitance C_s of the electrode is given by

$$C_n = \frac{\varepsilon S}{d}$$

where ε is the permittivity or dielectric constant of the solution, S is the surface area of the electrode/electrolyte interface, and d the thickness of the electrical double layer. Taking into account that d is generally less than 1 nm, the equation above shows immediately the technological advantage of supercapacitors over conventional capacitors, giving rise to specific capacitances of approximately 0.1 F/m^2. Moreover if a material of high specific surface area is used as the substrate for ion adsorption (active material), high values of capacitance can be reached[59].

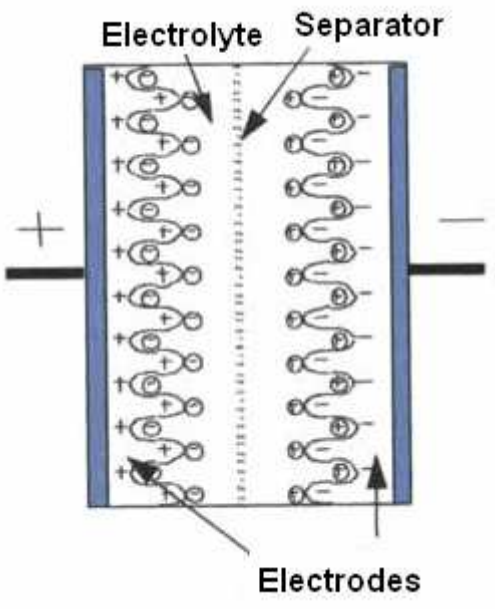

Figure 1.6 Schematic representation of an supercapacitor: + signs are cations of the electrolyte and – signs are anions of the electrolyte.

In a supercapacitor, the amounts of energy *W* accumulated is directly proportional to capacitance *C* and the square of voltage *U*

$$W = \frac{1}{2} CU^2$$

The stability interval of the electrolyte determines the operating voltage of the supercapacitor, but capacitance "*C*" depends mainly on the electrode material used. Organic electrolytes can make the supercapacitor easily operate in the range 2 to 2.5 V, while with ionic liquids it is even possible to extend this range to 3.5 - 4 V, although in aqueous solutions operating range usually demotes to 1 V. Thus, higher capacitance can be expected with organic electrolytes or ionic liquids for symmetric systems.

The main advantage of an electrochemical double-layer capacitor (EDLC) is its ability of high dynamic charge propagation that allows a rapid withdrawal of energy since the electrodes do not go into a phase transformation. The energy, the power *P*, of a supercapacitor is given by

$$P = \frac{U^2}{4R_s}$$

where R_s is the internal resistance, or in other words the equivalent series resistant (ESR). The ESR of the entire device is the sum of the resistances of all materials between the external contacts; substrate, active material, binder, separator, and electrolyte. Since the main function of supercapacitors is their use in high-power applications, it is essential to lower the series resistance by using high conductivity additives.

1. 3. 2. Conducting Polymers and Carbon Nanotubes for Supercapacitor Applications

When a supercapacitor charged, there is no chemical reaction takes place, the charging occurs as a concentration of electrons of the surface of the active material of the supercapacitor. As a result of this phenomenon, fast charging/discharging process, high electrical power and long lifetimes are promised. Taking this fact into account, it is clear that in order to have a supercapacitor with desirable properties, the active material should possess high surface area. There are three types of suitable material for a supercapacitor electrode: metal oxides, high surface-area activated carbons and conducting polymers.[64,65]

CP's are of interest in late years and they are promising materials for realization of high performance supercapacitors, as they are characterized by high specific capacitances, by high conductivities in the charged states and by fast charge-discharge processes. The charge processes pertain to the whole polymer mass and not only to the

surface[66]. These features suggest the possibility to develop devices with low ESR and high specific energy and power. However, the long-term stability during cycling is a major demand for an industrial application of CP's. Swelling and shrinkage of CP's, caused by the insertion/deinsertion of counter ions required for doping the polymer[67], is well known and may lead to degradation of the electrode during cycling. This obstacle has been over overcome to some level by using composite materials made of carbon materials such as CNT's or activated carbons with CP's. Carbon material in the bulk both ensures a good electrical conductivity even the CP is in its insulating state and improves the mechanical properties of the electrodes[67].

1. 4. Aim of the Study

As mentioned in the earlier chapters, using carbon nanotubes, CP's, or both as composites for the active material of the supercapacitor applications comes with some disadvantages as well as the advantages.

CP's although being a promising energy source for the job, lack the flexibility for insertion/deinsertion of the dopant ions resulting in shorter recycling life times than desired. CNT's are the employed to gain more flexibility however whether they are used as active materials solo, or engaged in a composite with a CP, they could not supply enough energy for the job.

Therefore, the objective of this study is, to obtain a new material for supercapacitor active material; by depositing a conducting polymer, polypyrrole, on to carbon nanotubes via electropolymerization. By this method, the problem of bulk charging in conducting polymers is aimed to be overcomed. Since the coating is in magnitudes of nanometers, only surface charging will exist, which is desirable for supercapacitor applications.

CHAPTER 2

EXPERIMENTAL

2.1. Materials

Pyrrole (Aldrich) and Lithium Perchlorate (Aldrich) were used without further purification. Acetonitrile (MeCN) were distilled over calcium hydride before use. All reactions were performed under argon atmosphere.

2.2. Instrumentation

2.2.1 Potentiostat

Electropolymerization was carried out with an Epsilon EC potentiostat/galvanostat, employing a three electrode system: working electrode, counter electrode and a reference electrode. Potentiostat keeps the voltage difference between working electrode and reference electrode at a constant value despite the changes in the current passing through the electrolytic cell, the concentration of the electroactive substance, and the solution resistance. The current supplied by the potentiostat can be determined by measuring the voltage drop across a resistance connected to the counter electrode in series. To compensate the changes in potential of working electrode, potentiostat continuously checks the potential of working electrode measured with respect to reference electrode, and changes the potential difference in between to maintain the desired potential value that was set.

2.2.2. Electrolysis Cell

Polymerization reactions were carried out in a one-compartment UV cell with three electrode configuration. Carbon nanofiber/ Cu plate/ Indium Tin Oxide-coated glass slide (7—50—0.6 mm, *R*s ≤10 Ω/□, Delta Technologies 306 Inc.) complex electrode is used as working electrode, a platinum wire as counter electrode, and a silver wire or 0.01M Ag/AgNO3 (Ag/Ag+) as reference. The electrolyte used was 0.1M of Lithium Perchlorate (LiClO4) in MeCN., and all potentials were reported with respect to the Ag wire.

2.2.3. Scanning Electron Microscopy

The morphologies of the polypyrrole coated on carbon nanofiber were analyzed using a Supra Gemini 35 VP Scanning Electron Microscope from Leo.

In the Scanning Electron Microscope (SEM) the area to be examined is irradiated with a finely focused electron beam, which may be static or swept in a raster across the surface of the specimen. The types of signals produced when the electron beam impinges on a specimen surface include secondary electrons, backscattered electrons, Auger electrons, characteristic X-Rays and photons of various energies. These signals are obtained from specific emission volumes within the sample and can be used to examine many characteristics of the sample such as composition, surface topography, crystallography, etc.

2.2.4. BET

BET theory is a well-known rule for the physical adsorption of gas molecules on a solid surface, that is basis for an important analysis technique for the measurement of the specific surface area of a material.

In 1938, Stephen Brunauer, Paul Hugh Emmett, and Edward Teller published an article about the BET theory in a journal[68] for the first time; “BET” consists of the first initials of their family names.

The concept of the theory is an extension of the Langmuir theory, which is a theory

for monolayer molecular adsorption, to multilayer adsorption with the following hypotheses: (a) gas molecules physically adsorb on a solid in layers infinitely; (b) there is no interaction between each adsorption layer; and (c) the Langmuir theory can be applied to each layer.

The specific area of polypyrrole coated on carbon nanofiber was analyzed using a Quanta Chrome NOVA 2200e adsorption isotherm instrument at 77 K. Before the experiments the samples were degassed under vacuum at 350°C for 12 hours. Surface area of the catalyst samples was determined by using Brunauer, Emmett and Teller (BET) method.

2.2.5. Solid State NMR

Solid-state NMR analyses cover a wide range of applications that cannot be addressed by liquid-state experiments. In solid-state NMR samples are place in 7mm diameter spinning rotors and spun at high speeds (3-14 kHz) in order to allow acquisition of NMR spectra with sufficient resolution to allow chemical determinations to be made.

The Polypyrrole/CNF samples were probed by ^{13}C MAS-NMR and ^{15}N MAS-NMR using an Inova 500 MHz NMR Varian System.

2.2.6. FTIR

Infrared spectroscopy is widely used in both research and industry as a simple and reliable technique for measurement, quality control and dynamic measurement. By measuring at a specific frequency over time, changes in the character or quantity of a particular bond can be measured.

2.3. Procedure

2.3.1. Synthesis of Carbon Nanofibers*

2.3.1.1. Catalyst preparation

A series of 3-d block metal based catalyst precursors were prepared (hydroxide, tartrate, and oxalate) by starting from chloride forms of metal salts were prepared both in the organometallic and oxide form by modifying the previously described methods [1] using Iron (Fe), Cobalt (Co), Nickel (Ni), Copper (Cu) and Zinc (Zn) as the catalyst metal.

The chloride salts of the metals were selected as the starting material and basic character of the solution was obtained by adding NaOH to the solution. Presence of the chloride and sodium ion in the saturated solution results with production of the NaCl, as a side product Eq 4.1.

$$\text{Metal-Cl} + \text{NaOH} + \text{Organic Acid} \longrightarrow \text{Metal-organic acid complex} + \text{NaCl} + H_2O$$

Eq 2.1.

Therefore, the support NaCl was produced while producing the organometallic or metal hydroxide catalyst precursor simultaneously. In order to keep the metal/support ratio in the range of 1/20 to 3/10, additional NaCl was added to the synthesis media during the synthesis of catalyst. The metal salt-sodium chloride mixture was exposed to vigorous mixing for 24 hours at room temperature, and then it is slowly evaporated at 50°C in 6 hrs. The final catalyst system was obtained in the pulverized form in which the active metal precursor particles were dispersed through the NaCl structure. The production scheme of the catalysts can be seen in Figure 4.1.

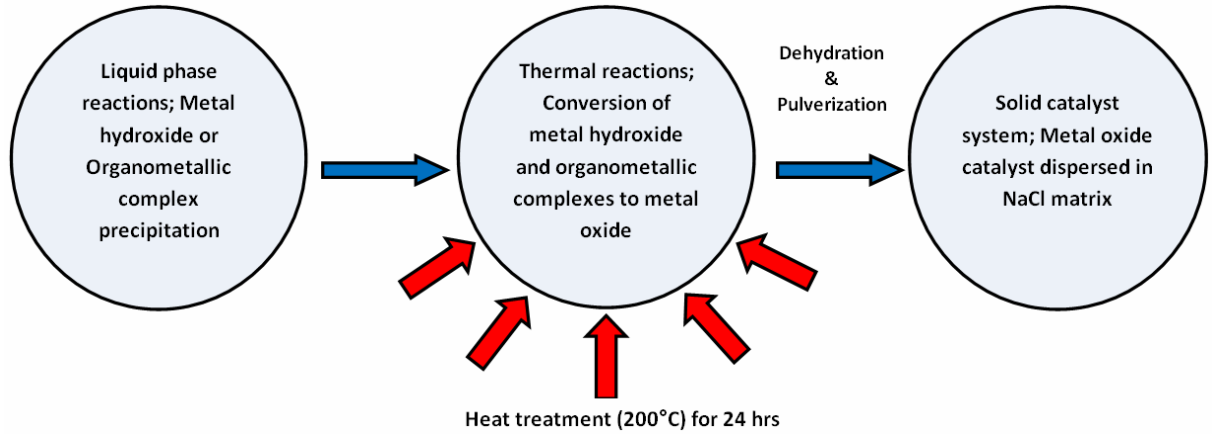

Figure 2.1 Production scheme of the catalysts

In order to obtain a mono dispersed and stable sized catalyst, the catalyst-NaCl support system was exposed to mechanical activation between 12-24 hrs using a ball-mill system with 125 ml vial together with zirconium balls 10 mm in diameter. The effect of mechanical mixing on the size and dispersion of the metallic particles has been investigated for different purposes previously [2-4]. Mechanical activation using a ball-mill system reduces the particle size of the catalyst and gives the catalyst a uniform particle diameter distribution.

Other than chloride salts, nitrate and sulfate salts of metals were used as starting material for the preparation of the catalysts as well. The same procedures were applied for the preparation of the catalysts and the differences between the catalysts which were prepared starting chloride salts and the nitrate or sulfate salts such as the particle size, dispersion and the effect on CNT/CNF formation were compared.

2.3.1.2. Carbon nanofiber and nanotube production

2.3.1.2. a. Optimization of the growth conditions

Carbon nanofiber and carbon nanotube production attempts have been performed by using conventional CVD set-up Figure 4.2. The catalyst system was placed in to the quartz tube reactor with a diameter, Φ= 30 mm and length, L= 90 cm. The system was kept at 500°C for 30 min under Ar flow for the stabilization of the catalysts, and then hydrogen gas was passed through the tubular reactor in order to

reduce the catalyst into the metallic form. After the catalyst system prepared for the production of carbonaceous material, high purity acetylene was started to flow for the formation of the carbon nanostructures.

In order to optimize the growth conditions, a series of CVD experiments were performed. In the CNT synthesis process, four control factors (growth parameters) were examined;

1. Furnace temperature (between 500 and 700, 800 °C),
2. Flow rate of the acetylene (0.5, 1.0, 2.0 and 3.0 L/min),
3. Metal catalyst concentration (between 1 and 30 wt%)
4. Nature of the catalyst.

Subsequently, the performance of the catalysts was evaluated according to the three criteria;

1. Total mass of the product
2. Diameter of the fibers/tubes
3. Length of the fibers/tubes

The change in the parameters and CVD conditions were summarized in table 4.1.

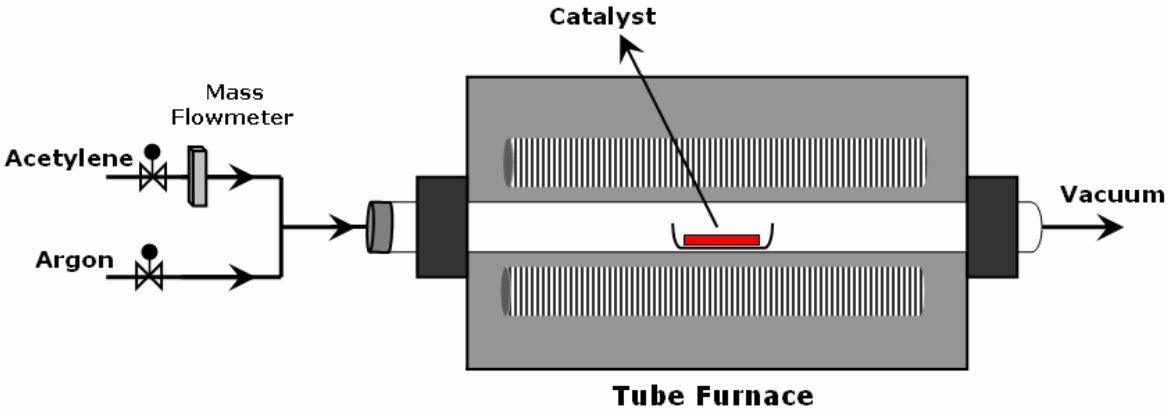

Figure 2.2 CVD process set-up for carbon nanostructure production

2.3.1.2. b. Kinetic Studies

In the kinetic studies section, an experimental work on the kinetics of the CNT/CNF growth was performed that determines general reaction rate of carbon nanotube synthesis from acetylene as carbon source on the organometallic catalyst/NaCl system as a function of operating conditions in the CVD reactor. First, temperature dependent growth of the CNT/CNF was investigated and an efficieny curve for each catalyst obtained, Table 4.2., summarizes these experiments. After determination the most efficient temperature for each catalyst, the time dependent kinetic studies were performed at the most efficient temperature for each catalyst. The yield of the reaction was calculated according to the equation 4.2., and the performance of the catalysts was compared with the ideal gas equation 4.3. The experimental founding was obtained by the use of a mass flowmeter and ideal gas equation and comparing the reaction yield with the calculated yields.

$$\text{Product yield} = \frac{(Wf - Wc)}{Wc} \text{ x100\%} \qquad \text{Eq 2.2.}$$

Where;

Wf = final weight of the product and catalyst together

Wc = weight of the catalyst after reduction step

$$PV = nRT \qquad \text{Eq 2.3.}$$

In equation 4.3., the “n” value was calculated and the variables were used as;

P = pressure (760 mmHg)

V = volume was calculated according to the reaction time and mass spectrometer

n = moles of gas 0.082 L atm mol $^{-1}K^{-1}$

R = gas constant

T = temperature (K)

2.3.2. Deposition of Polypyrrole on Carbon Nanofibers

2.3.2.1. Preparation of the Working Electrode

In the deposition process of Polypyrrole on to CNF's, a complex sandwich electrode is employed as the working electrode.

An Indium Tinoxide coated glass slide is used as a template for the working electrode. A two-sided sticky copper plated is fixated onto the conducting side of the ITO slide. Then, while weighing, 50 mg CNF is put on to the sticky copper plate carefully and distributed evenly so as to cover the plate completely.

2.3.2.2. Deposition

The deposition of Polypyrrole onto CNF is carried out in 0.1 M $LiClO_4$ dissolved in MeCN. A three electrode electrolysis configuration is set in an one compartment UV cell. The working electrode is prepared as described above; a Pt wire is used as counter electrode and an Ag wire is employed as the reference electrode. The electrodeposition was performed from a $1.16x10^{-2}$ M solution of the monomer in the electrolyte potentiodynamically at a scan rate of 25 mV/s. The cell has gas inlets to pass the N_2 gas through the solution in order to achieve inert medium and to prevent the oxidation during the electrolysis.

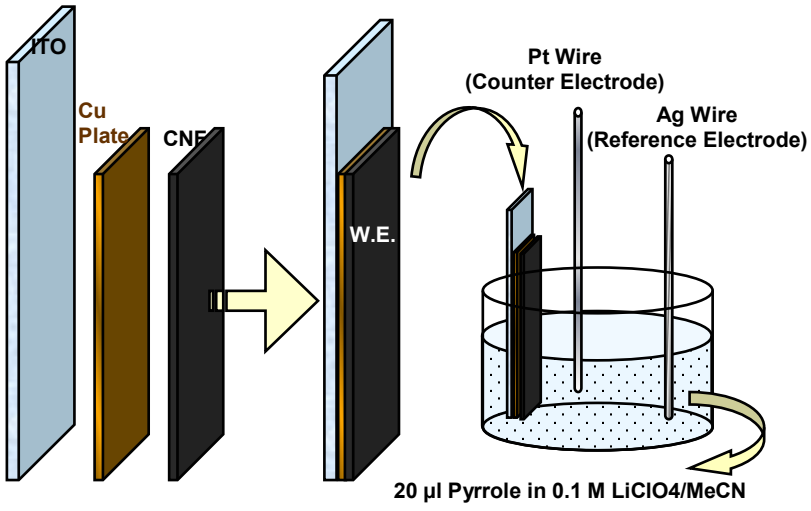

Figure 2.3 A schematic representation of the electrolysis cell.

CHAPTER 3

RESULTS and DISCUSSION

Optimization

3.1.1. Optimization of the Number of Cycling

During the optimization process of the Polypyrrole coating on the CNF's, the most important factor was to decide how much polymer should be deposited on the CNF's. As described in the aforementioned chapters, there are two main factors to have a desirable active material candidate for supercapacitor applications. First, the charge deposition should take place at the surface of the active material rather than in the bulk. Looking at this supposition, one can dare to decide that a thinner layer should be constructed to guarantee not having charge deposition in the bulk of the CP. On the other hand it is crucial that the active material possess high specific capacitance to be a good candidate for the application which could be easily provided by more conducting polymer deposition. Hence, the active material was needed to be optimized by means of the deposition amount of the conducting polymer on to CNF's.

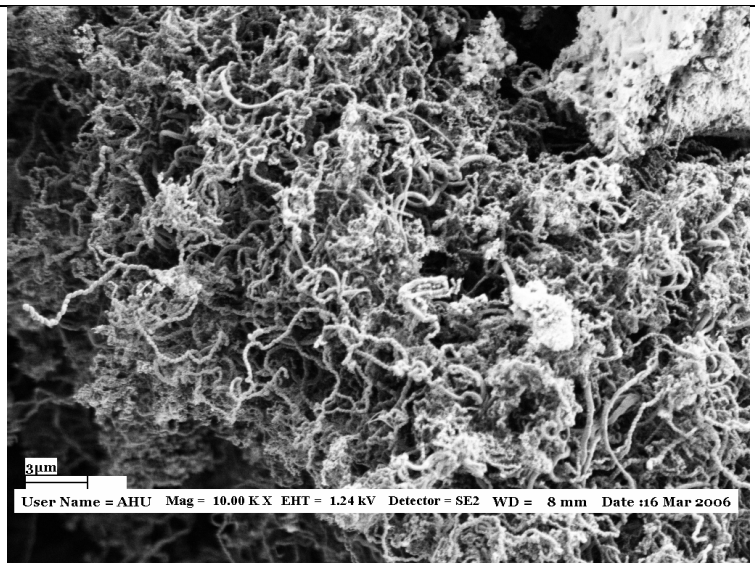

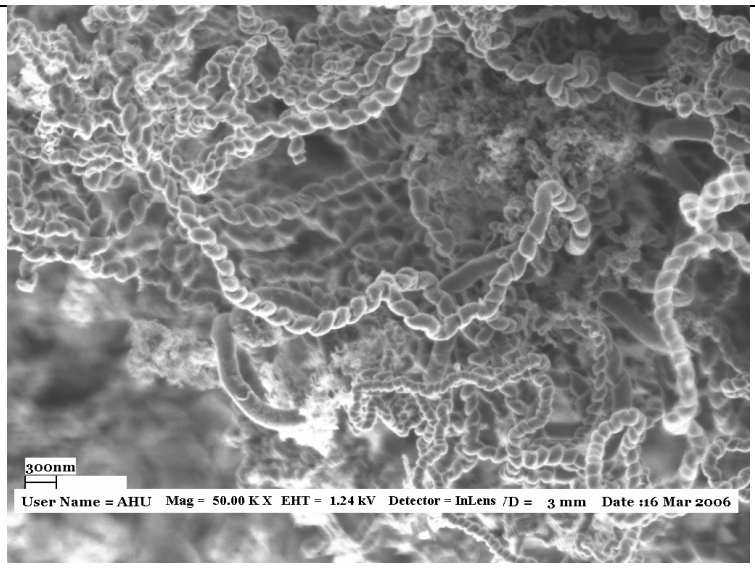

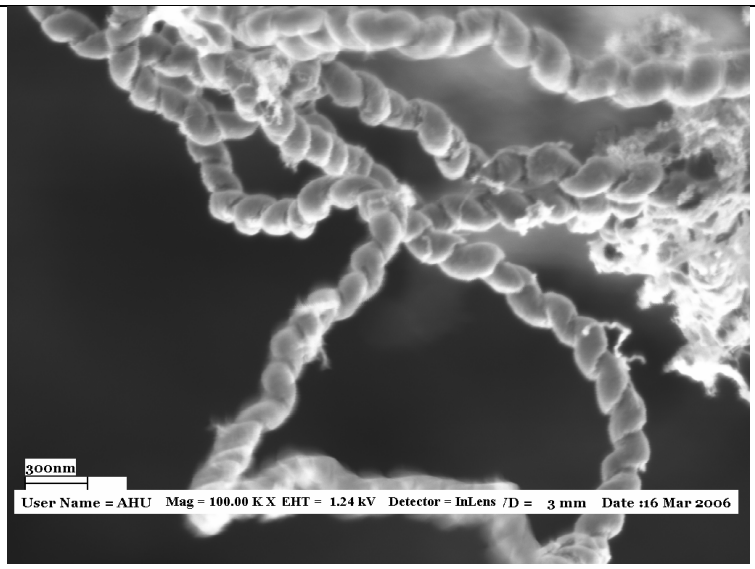

Figure 3.1 SEM images of uncoated CNF's used as a template for PPy

a)

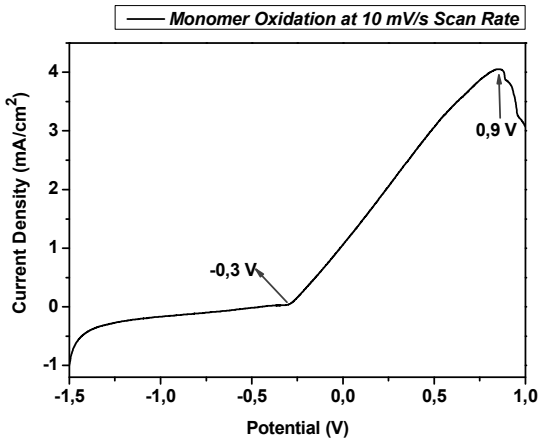

b)

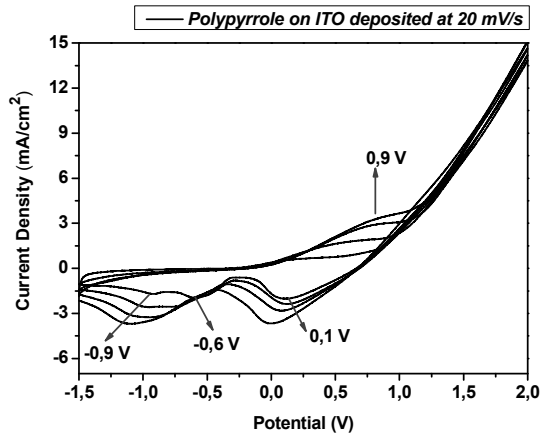

c)

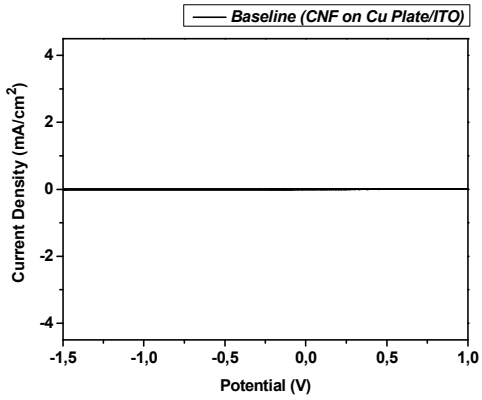

Figure 3.2 The voltammograms of a) Polypyrrole on ITO, b) baseline of the CNF/Cu plate/ITO electrode, and c) monomer oxidation of Polypyrrole on CNF.

Figure 3.1 shows the SEM images of uncoated CNF's. As seen above, the CNF's are twisted before coating, therefore SEM images directly proves if the CNF's are coated successfully after polymerization.

In pyrrole monomer oxidation on ITO voltammogram shown in Figure 3.2.(a) the onset potential read as -0.3 V which expresses the starting point of the oxidation and oxidation potential is 0.9 V as directed on the voltammogram also. According to this information, the electropolymerization of pyrrole can be done. Figure 3.2.(b) shows a regular cyclic voltammogram of polypyrrole on ITO electrode. There can be seen one oxidation peak at 0.9 V and three reduction peaks at 0.1 V, -0.6 V and -0.9 V which the latter two eventually diffuse in to one peak.

First the constructed complex electrode was investigated whether it went under any oxidation and/or reduction reaction. It was seen that the electrode was available to employ only between the potentials (-2 V) – (+2 V). Figure 3.2.(c) shows the baseline voltammogram in between the working range of the carbon nanofiber templated polypyrrole which is (-1,5 V) – (+1 V). The fact that the voltammogram shows no peak is proving that all peaks during deposition belong to PPy.

Figure 3.3 shows the monomer oxidation voltammogram of carbon nanofiber templated polypyrrole (CNF templated PPy). This graph act as a lamppost for the further analysis since has the information about electropolymerization range, onset potential and oxidation potential, which are also pointed at the voltammogram as -0.30 V and as 0.85 V consequently.

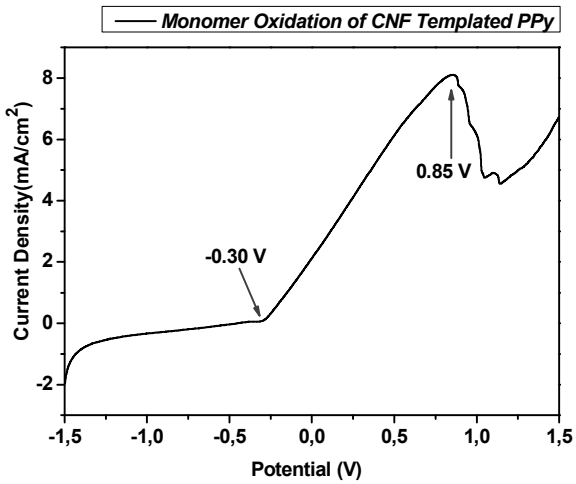

Figure 3.3 Monomer oxidation voltammogram of CNF templated PPy.

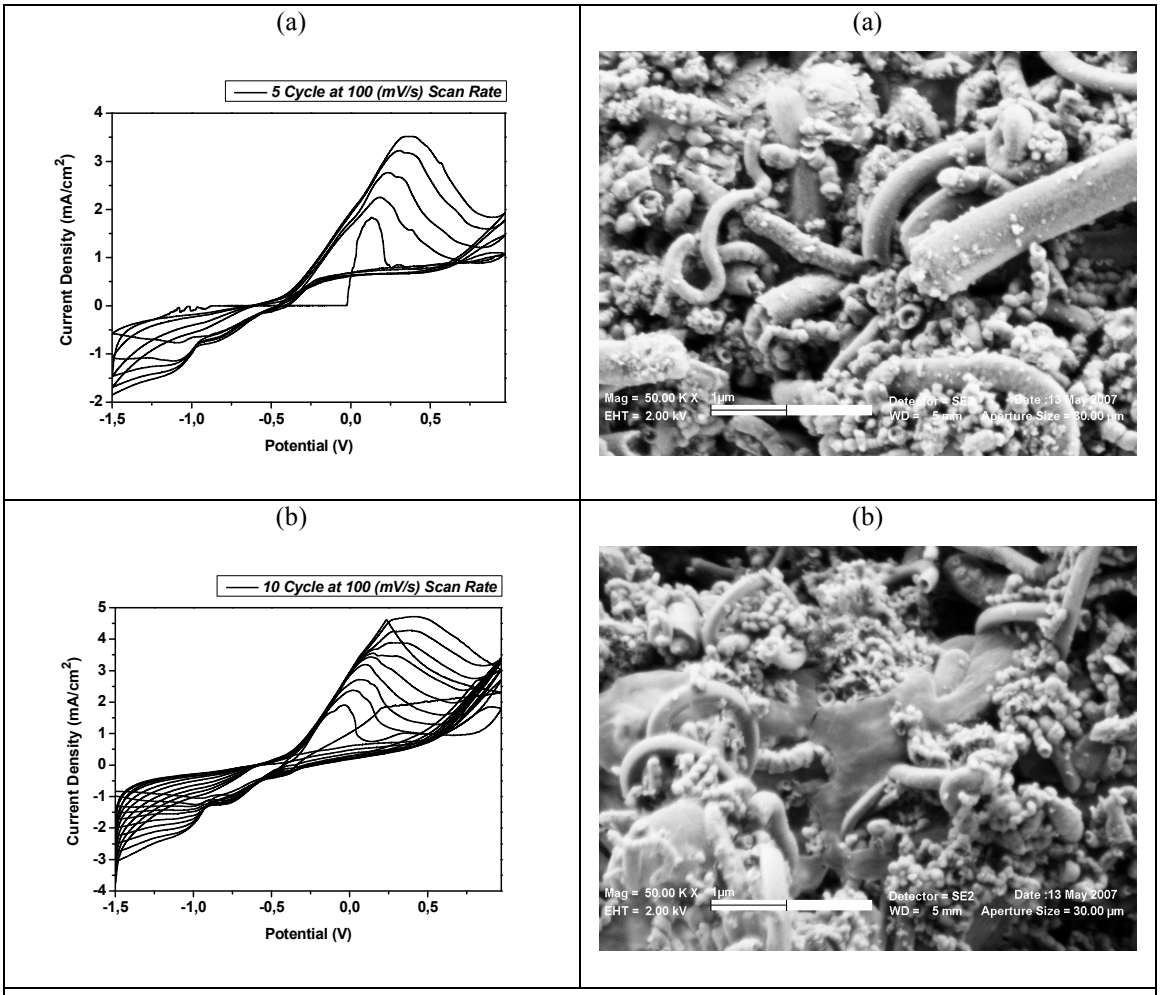

Figure 3.4. Two voltammograms of CNF templated PPy with different amounts of deposition and their consequent SEM images: (a) 5 times cycled (b) 10 times cycled.

During the optimization process, the first batches were the ones that 5 times cycled and the one that was 10 times cycled. Figure 3.4 shows the voltammograms of CNF templated Polypyrrole samples that are 5 times cycled (a), and 10 times cycled (b) and the correlating SEM images showing 50 times magnified version of them. The specific capacitance of the samples are calculated by integrating the area of the outermost cycle in voltammogram and it is found as 0.0129 C/cm^2 for the first one and 0.0227 C/cm^2 for the latter one. From this result it can be stated that the specific capacitance of the sample increases by the increasing amount of deposition. However, from SEM images, it is obvious that as the number of the cycling is increased, not only the surface of the CNF's are coated but also there has been block polymers in between the fibers which is not a

desirable outcome for supercapacitors in two aspects as explained before: the diminution of the surface area and the capacitance accumulated in the bulk.

In order to find out after which cycle this agglomeration starts, a series of cyclic voltammogram experiments was employed.

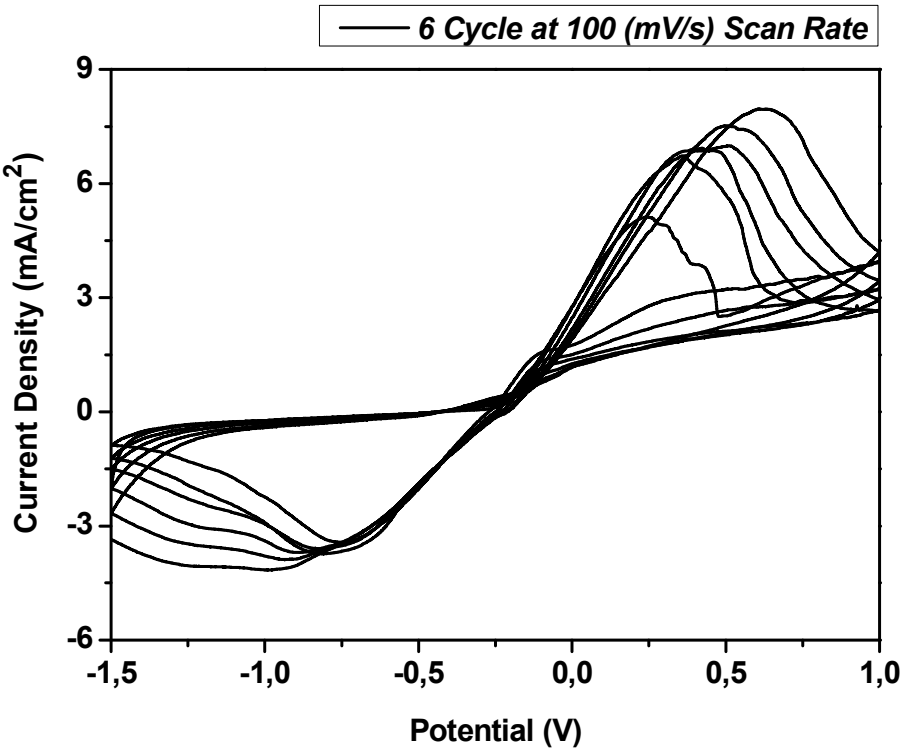

Figure 3.5 Voltammogram and SEM image of CNF templated PPy via 6 times cycling

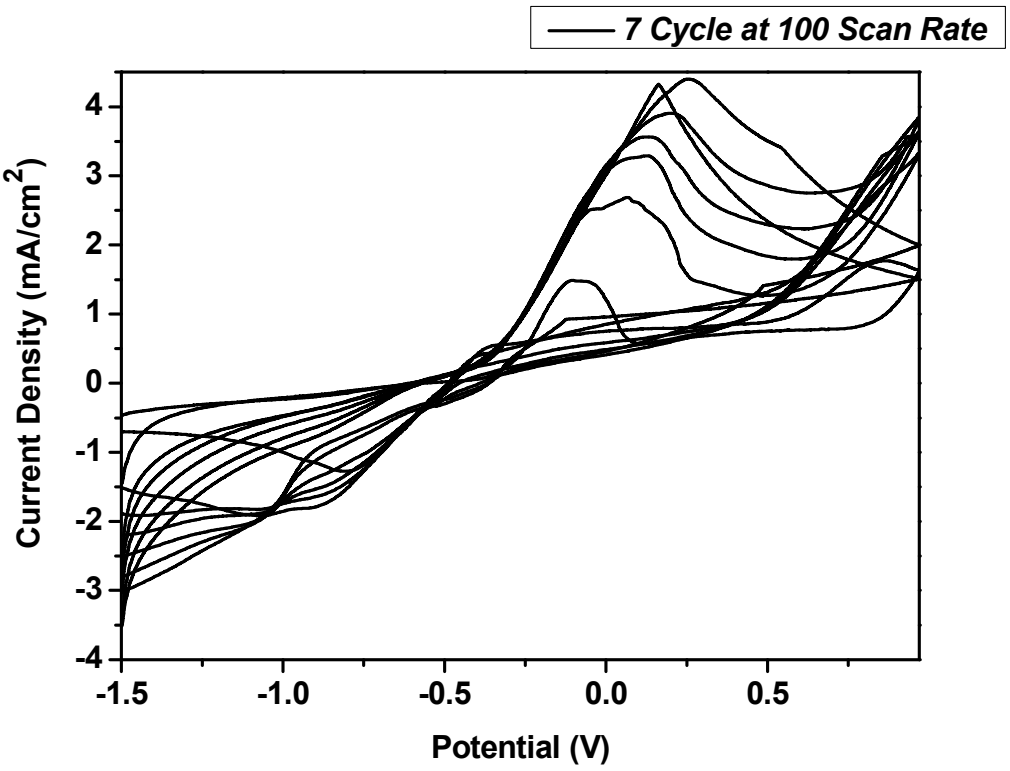

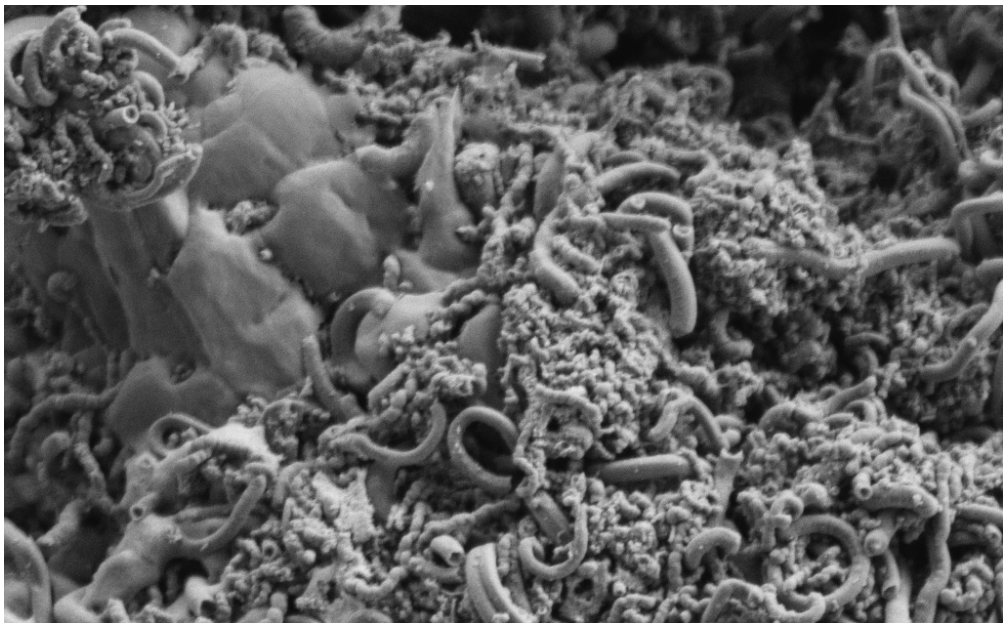

Figure 3.6 Voltammogram and SEM image of CNF templated PPy via 7 times cycling at 100 mV/s scan rate.

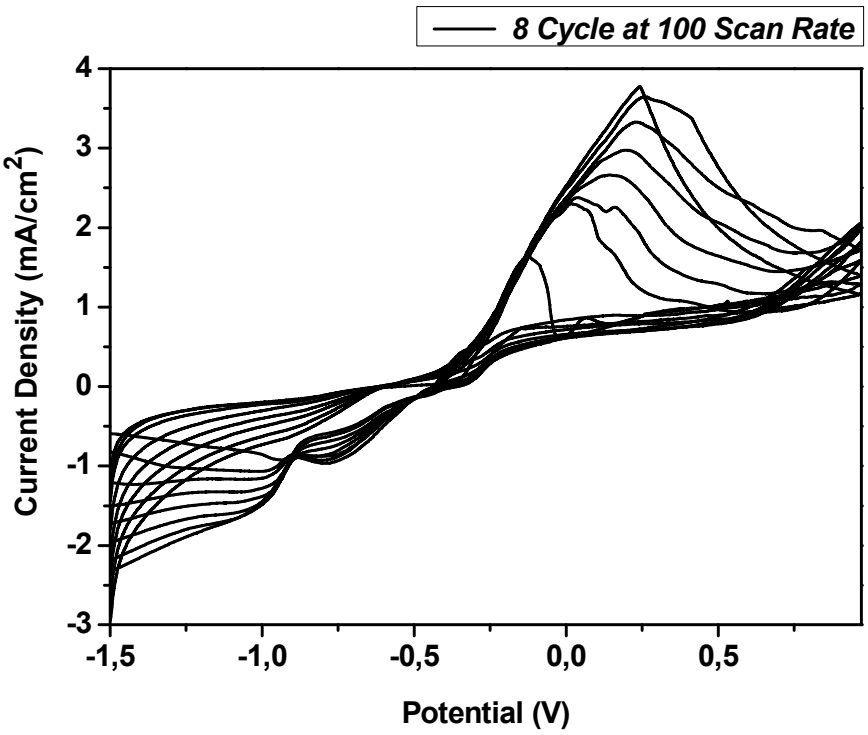

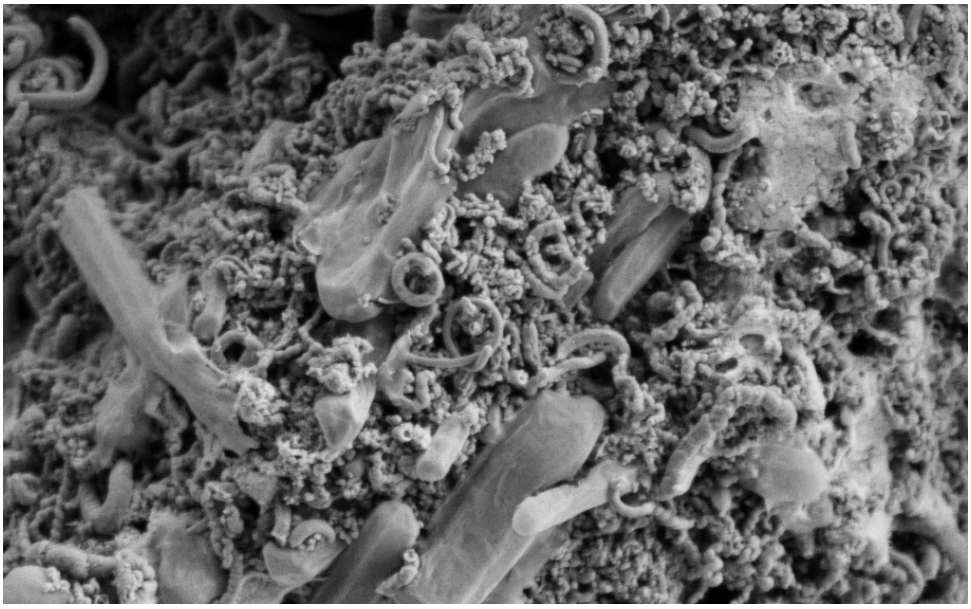

Figure 3.7 Voltammogram and SEM image of CNF templated PPy via 7 times cycling at 100 mV/s scan rate.

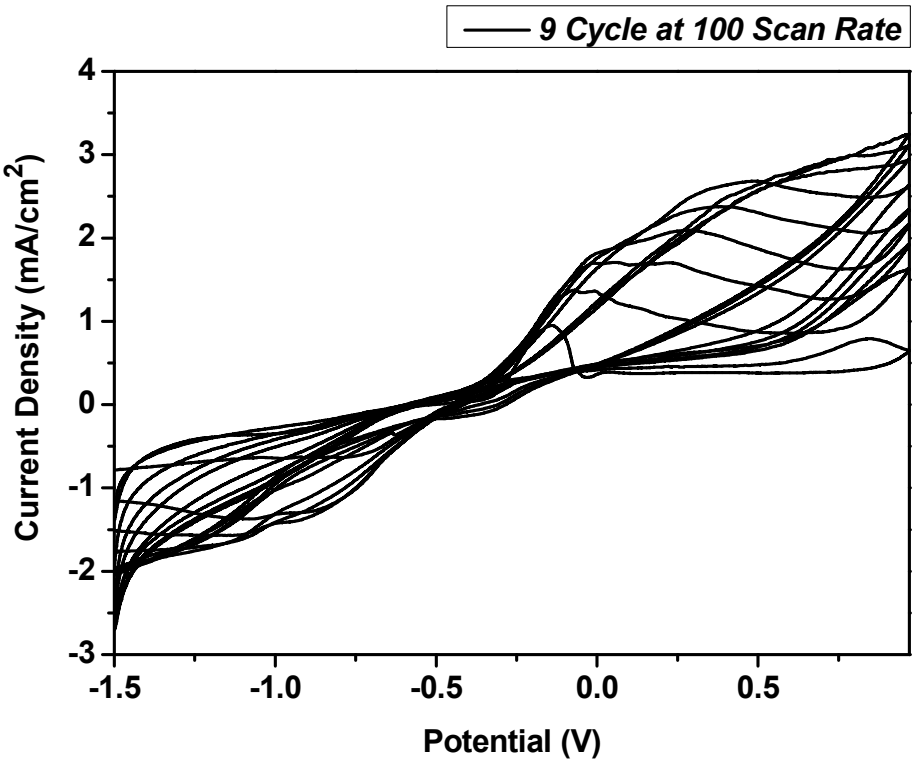

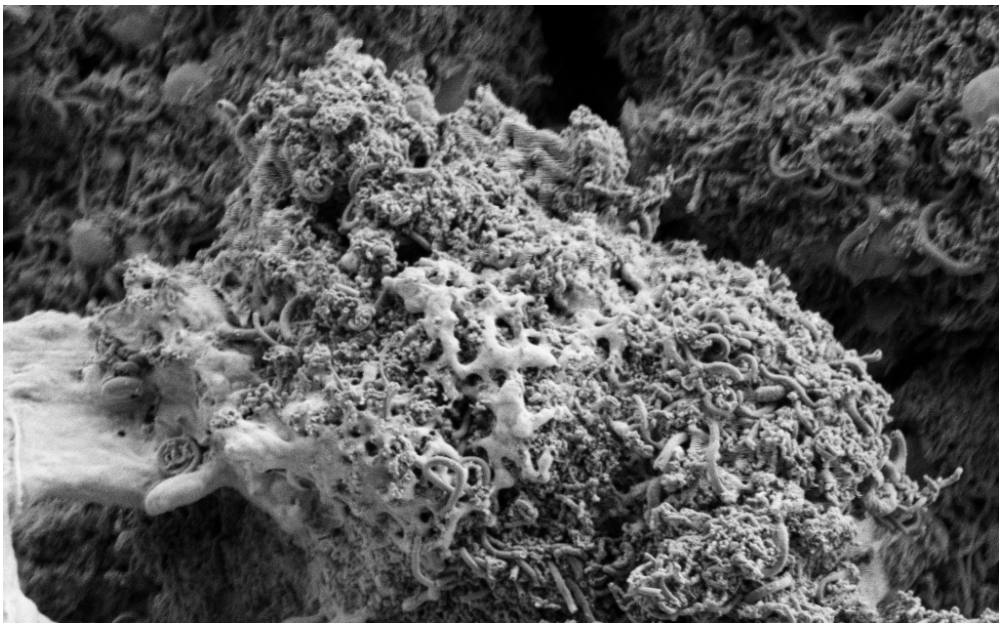

Figure 3.8 Voltammogram and SEM image of CNF templated PPy via 7 times cycling at 100 mV/s scan rate.

In Figures 3.6, 3.7, 3.8 and 3.9; there are voltammograms and the corresponding SEM images for a range of cycling times differing between 6 and 9 at the same scan rate; 100 mV/s. The specific capacitance values of the samples increase with the increasing amount of deposition as suggested before. The capacitance values for 6, 7, 8 and 9 times cycled polymer are consequently 0.0133 C/cm^2, 0.0147 C/cm^2, 0.0172 C/cm^2, and 202 C/cm^2. Therefore, unless the blockage of polymers had occurred in the high deposition sampled, it could have been concluded that the more the sample is deposited via cycling the better active material is synthesized. However, SEM images prove that the block polymer free samples can be obtained only until the 6th cycle. The block polymerization starts at the 7th cycle and gets more and more as the cycling continues. In fact the block polymerization gets so high by the 9th cycle, it is not only in-between the PPy coated CNF's, but also on them making the surface area even smaller.

3.1.2. Optimization of the Scan Rate

In the second stage of the optimization, the goal to be accomplished was to redound the deposition amount without having blocks of polymers in the sample. Since it is known from the former experiments that the blocking starts right after the 6th cycle, there were two possible solutions:

i. higher the deposition amount by using slower scan rates while cycling 6 times, in orders to have thicker polymer coating on CNF's meanwhile preventing the block polymerization, or;

ii. lower the deposition amount by using faster scan rate while cycling 7 times so as not to have the block polymers in-between the fibers.

To continue optimizing by using the aspects described above, first 25 mV/s, 50 mV/s and 75 mV/s scan rates are experienced for the 6 times cycled samples.

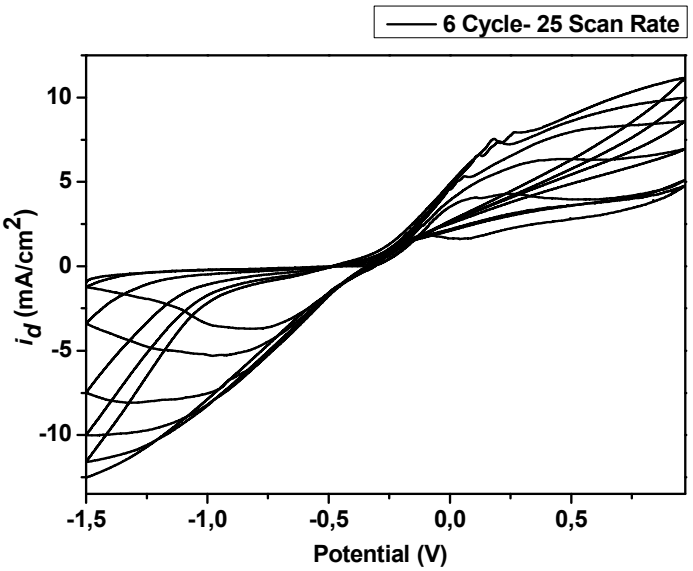

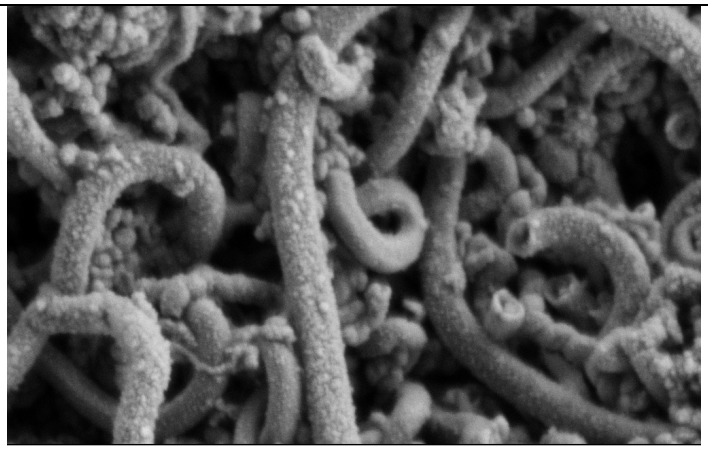

Figure 3.9 The voltammogram of CNF templated PPy deposited via 6 times cycling at a scan rate of 25 mV/s, and its SEM images: (b) 20000 times magnified (c) 50000 times magnified.

(a)

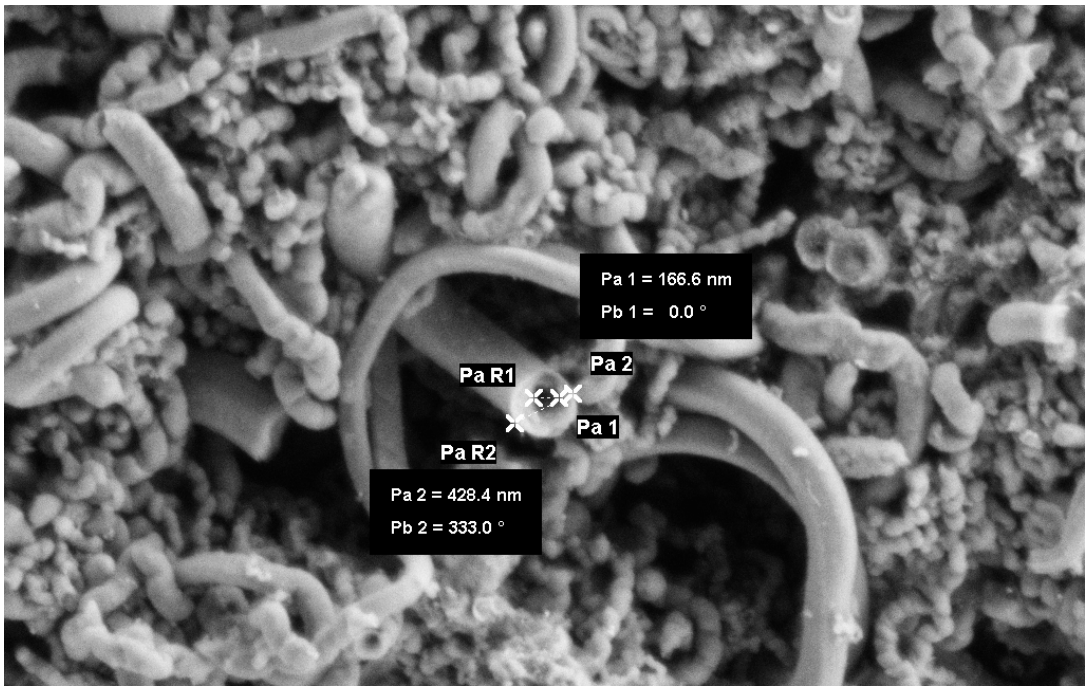

(b)

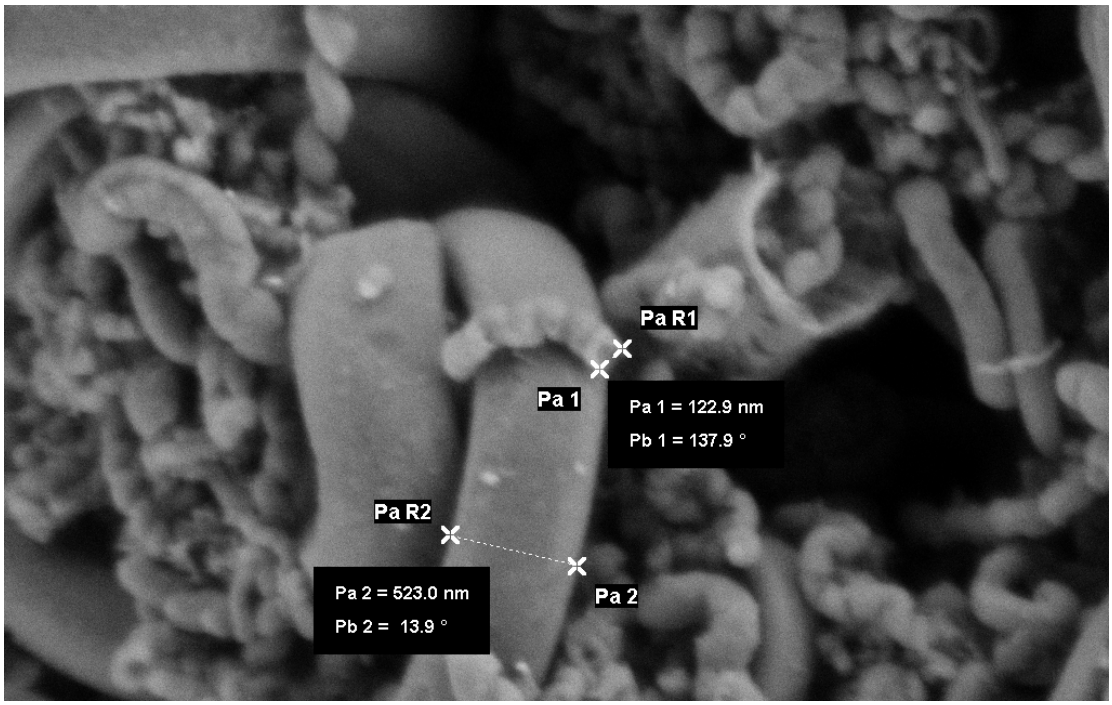

Figure 3.10 SEM images of 6 times cycled CNF Templated PPy (at 25 mV/s scan rate): (a) 50000 times magnified (b) 100000 times magnified.

A successful deposition was obtained via scanning at 25 mV/s by 6 cycles whose voltammogram and SEM images are displayed in Figure 3.9. With this sample, the specific capacitance value has shown a drastic increase and found as 0.0276 C/cm^2, since the sample which was also cycled 6 times but at the scan rate of 100 mV/s posses the specific capacitance value 0.0133 C/cm^2.

Looking closer to samples (Figure 3.10b), it can be observed that there are fewer uncoated CNF's when compared to the one deposited at 100 mV/s scan rate, which results in the outcome mentioned in the paragraph above. The deposited PPy thickness differentiates between 300-400 nm, supplies successful amount of surface for charge deposition but not for bulk deposition, which is a situation desired for supercapacitor active materials. The sample surface area was founded as 600 m^2/g from BET calculations.

The capacitance value for the sample, which was deposited with 50 mV/s scan rate, is found as 0.0166 C/cm^2 and is smaller than the former sample. Also the SEM images shows that there is less homogeneity between the PPy thicknesses of the coated CNF's and there are more uncoated CNF's when compared to the sample prepared via depositing at 25 mV/s scan rate (Figure 3.11).

Figure 3.12a shows the voltammogram and the SEM images of the sample deposited at 75 mV/s scan rate, whose specific capacitance is 0.0151 C/cm^2. This sample shows the lowest specific capacitance among other samples which are coated 6 cycles. The SEM images shown in Figure 3.12b and 3.12c reveals that more CNF's are stayed uncoated when compared to the former sample which may be the cause of the decrease in the specific capacitance.

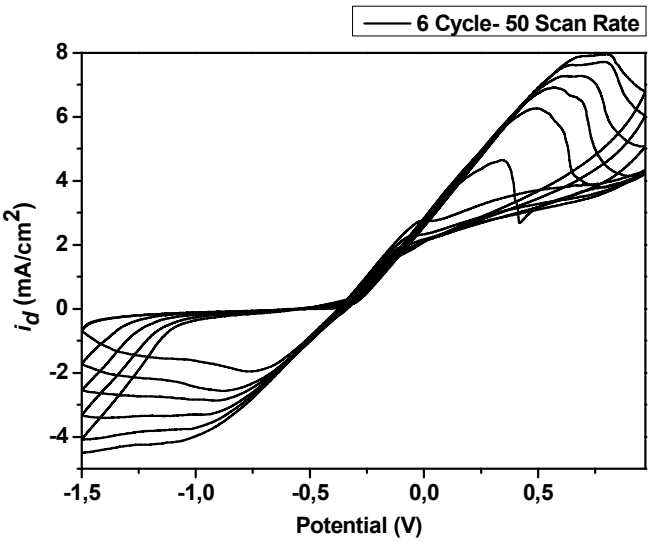

Figure 3.11 The voltammogram of CNF templated PPy deposited via 6 times cycling at a scan rate of 50 mV/s, and its SEM images: (b) 20000 times magnified (c) 50000 times magnified.

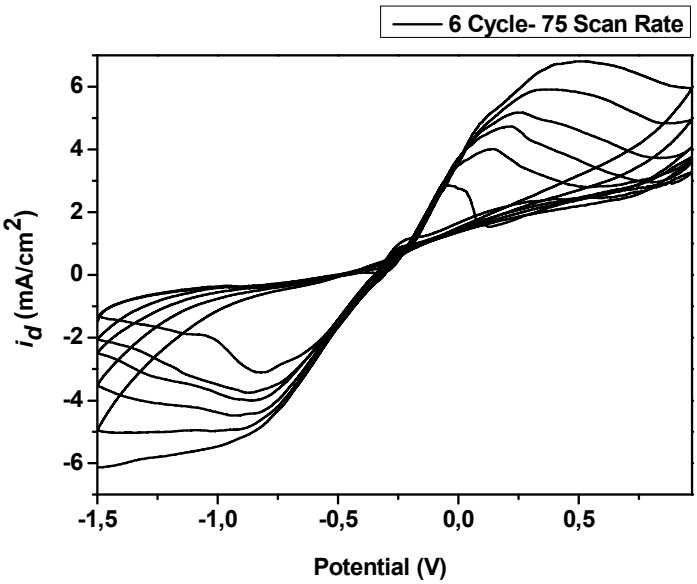

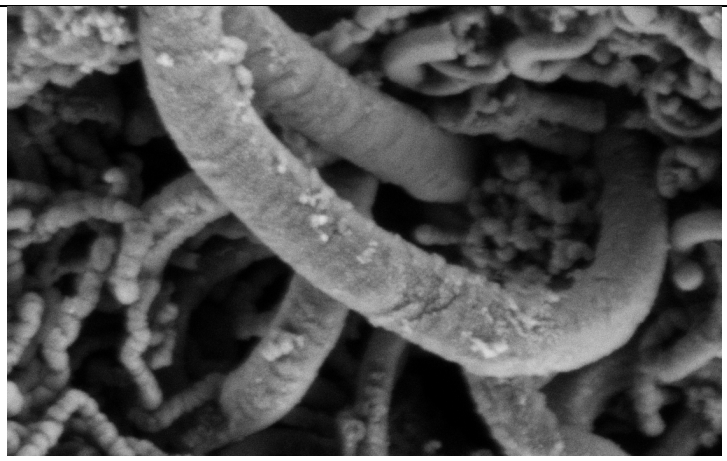

Figure 3.12 The voltammogram of CNF templated PPy deposited via 6 times cycling at a scan rate of 75 mV/s, and its SEM images: (b) 20000 times magnified (c) 50000 times magnified.

After examining the effects of different scan rates on the 6 times cycled CNF templated PPy samples, the scan rate difference effect was observed on the 7 times cycled samples.

For the 7 times cycled samples, two different scan rates were analyzed. The voltammogram and the SEM images of the sample scanned at 150 mV/s scan rate are displayed in Figure 3.13. The specific capacitance of the sample, calculated by integrating the area of the last full scan of the cyclic voltammogram, is 0.0208 C/cm^2 which is higher than the 7 times cycled sample at 100 mV/s scan rate, whose specific capacitance was calculated as 0.0147 C/cm^2. This sudden increase is most likely the result of not having blocks of PPy unlike the sample scanned at 100 mV/s. Therefore it is clear that the presumption that is made at the beginning of the optimization is proven correct. When the scan rate is increased, the block polymerization is prevented resulting in the increase of specific capacitance. However the specific capacitance of the sample deposited by 7 times cycling at 150 mV/s scan rate is not as high as the sample's deposited by 6 times cycling at 25 mV/s scan rate.

Figure 3.14 shows the voltammogram and the SEM images of the sample scanned at 200 mV/s. The specific capacitance of this sample is calculated as 0.0167 C/cm^2, lower than the former sample as expected.

Figure 3.15 is the SEM image of the sample deposited by 7 times cycling at 200 mV/s scan rate, 50000 time magnified. As clearly seen, the homogeneity of the thickness of the PPy coated CNF's is completely lost and there are many CNF's stayed uncoated, resulting in decreasing of the specific capacitance of the sample. Also the thickest PPy coated CNF is measured as ~150 nm, whereas the sample deposited by 6 times cycling at 25 mV/s scan rate was measured as ~400 nm.

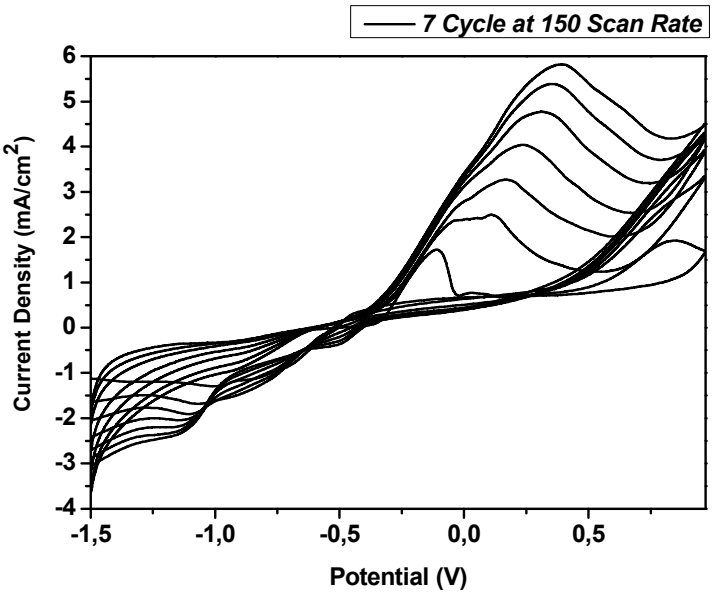

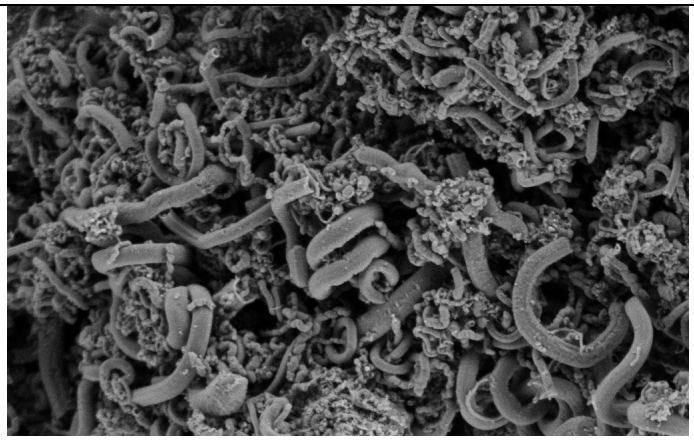

Figure 3.13 The voltammogram of CNF templated PPy deposited via 7 times cycling at a scan rate of 150 mV/s, and its SEM images: (b) 20000 times magnified (c) 50000 times magnified.

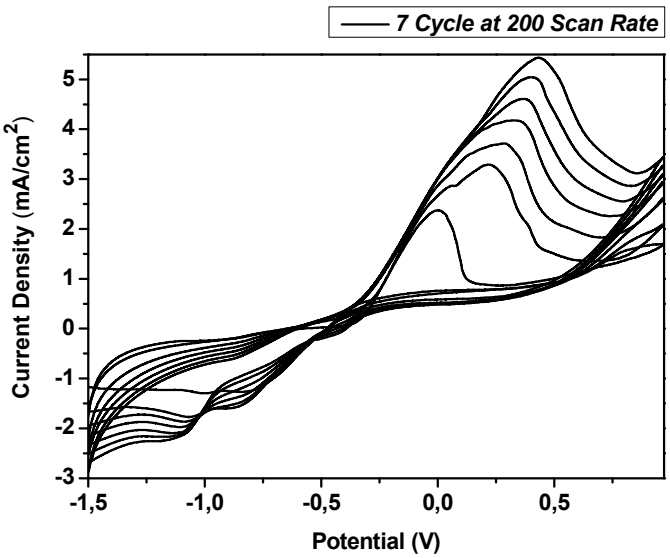

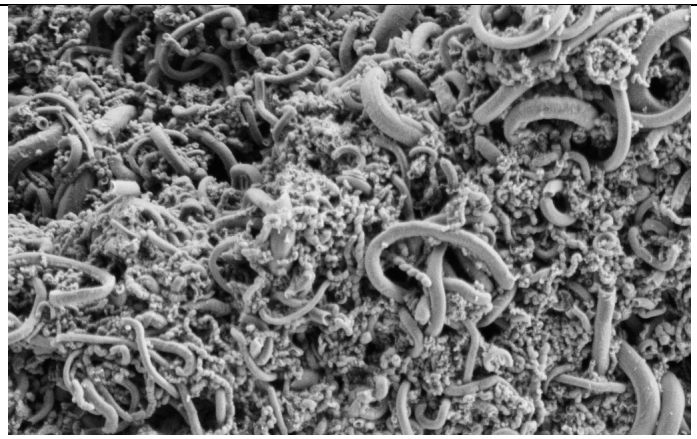

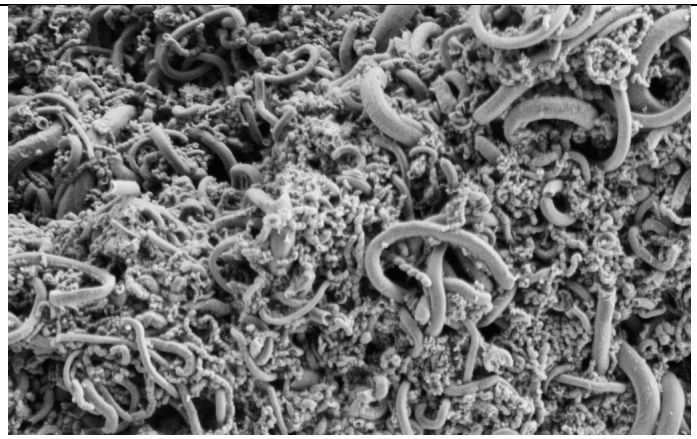

Figure 3.14 The voltammogram of CNF templated PPy deposited via 6 times cycling at a scan rate of 200 mV/s, and its SEM images: (b) 20000 times magnified (c) 50000 times magnified.

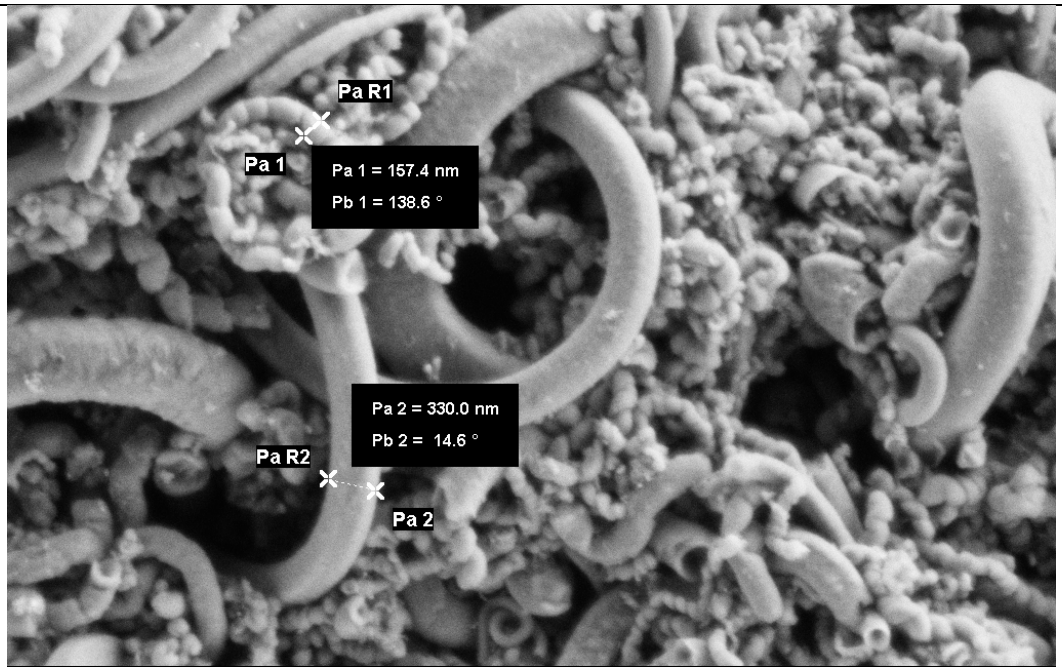

Figure 3.15 The SEM image of CNF templated PPy deposited via 6 times cycling at a scan rate of 200 mV/s, 50000 times magnified.

3. 2. Characterization

3. 2. 1. NMR

Two different types of nuclear resonance spectroscopy is used in characterizing the CNF templated PPy samples.

3. 2. 1. a. C^{13} NMR Spectroscopy

C^{13} NMR spectroscopy is used in order to analyze the coating on the CNF's whether it is PPy deposition or not. A PPy sample is composed of infinitely many chains with every monomer containing two –CH2 groups and two –CH groups adjacent to a –NH functional group.

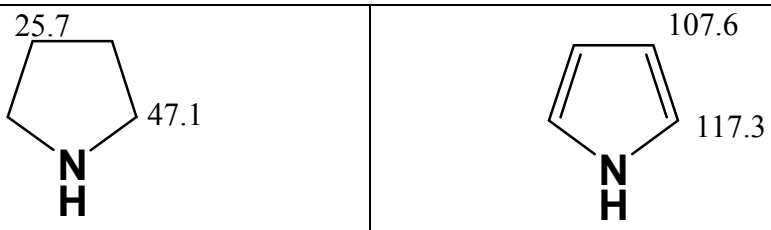

Figure 3.16 NMR shifts of (a) Pyrrolidine, (b) Pyrrole

NMR shifts of pyrrolidine and pyrrole are given in Figure 3.16[69]. Although the NMR of PPy is expected to have peaks at about ~100 nm, in the CNF templated PPy NMR spectrum differs between ~40nm - ~100 nm. This difference may arise from the fact that the electron moiety that shields the compound is now delocalized over a much bigger molecule; hence NMR values are expected to shift towards high area having a diamagnetic shift (Figure 3.17).

3. 2. 1. a. N^{15} NMR Spectroscopy

Looking at the N^{15} NMR spectrum (Figure 3.18) shows some broad peaks about ~200 ppm and ~300 ppm indicating the presence of N atom in the sample.

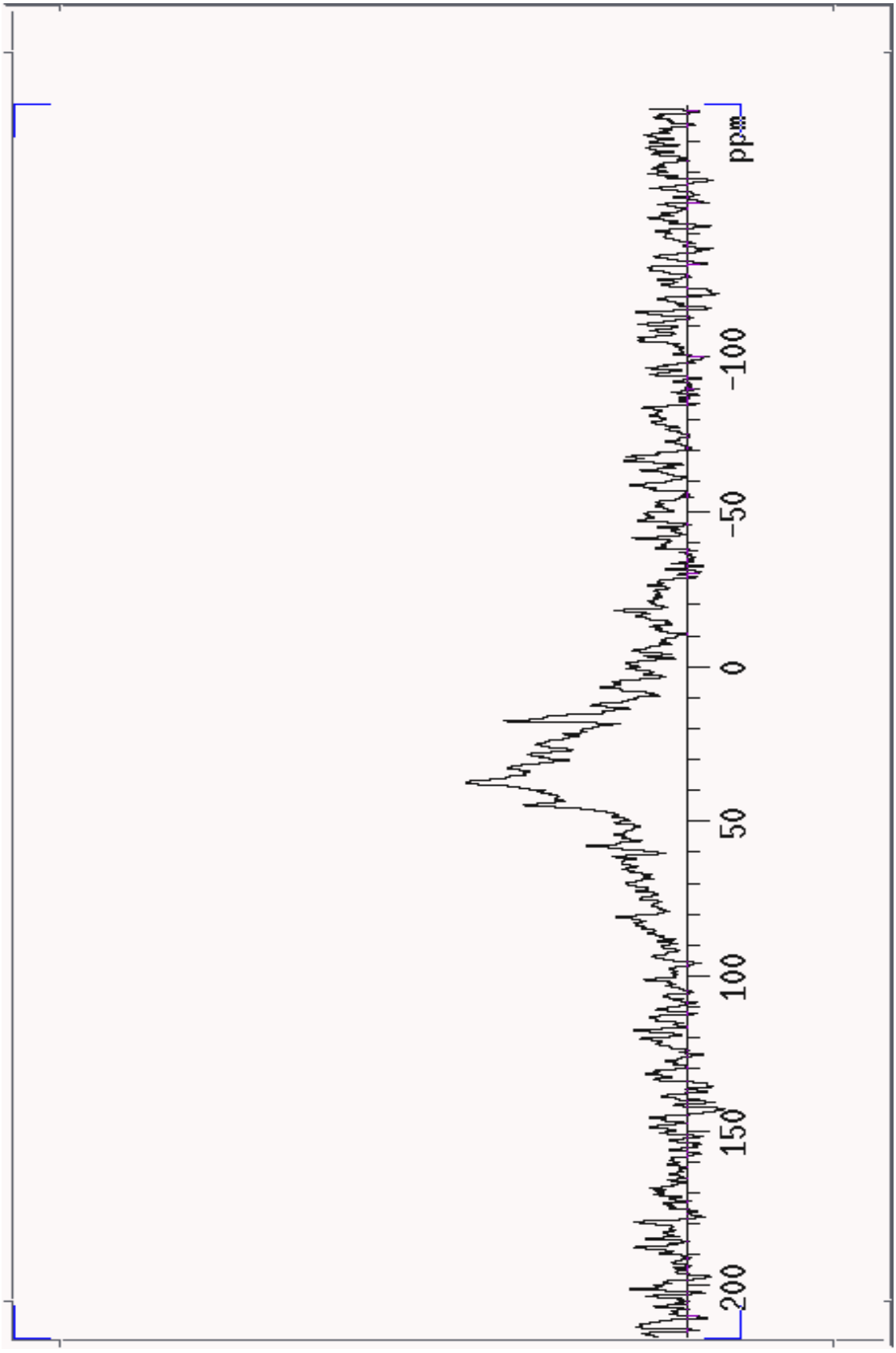

Figure 3.17 C13 NMR of CNF templated PPy deposited via 6 times cycling at 25 mV/s scan rate.

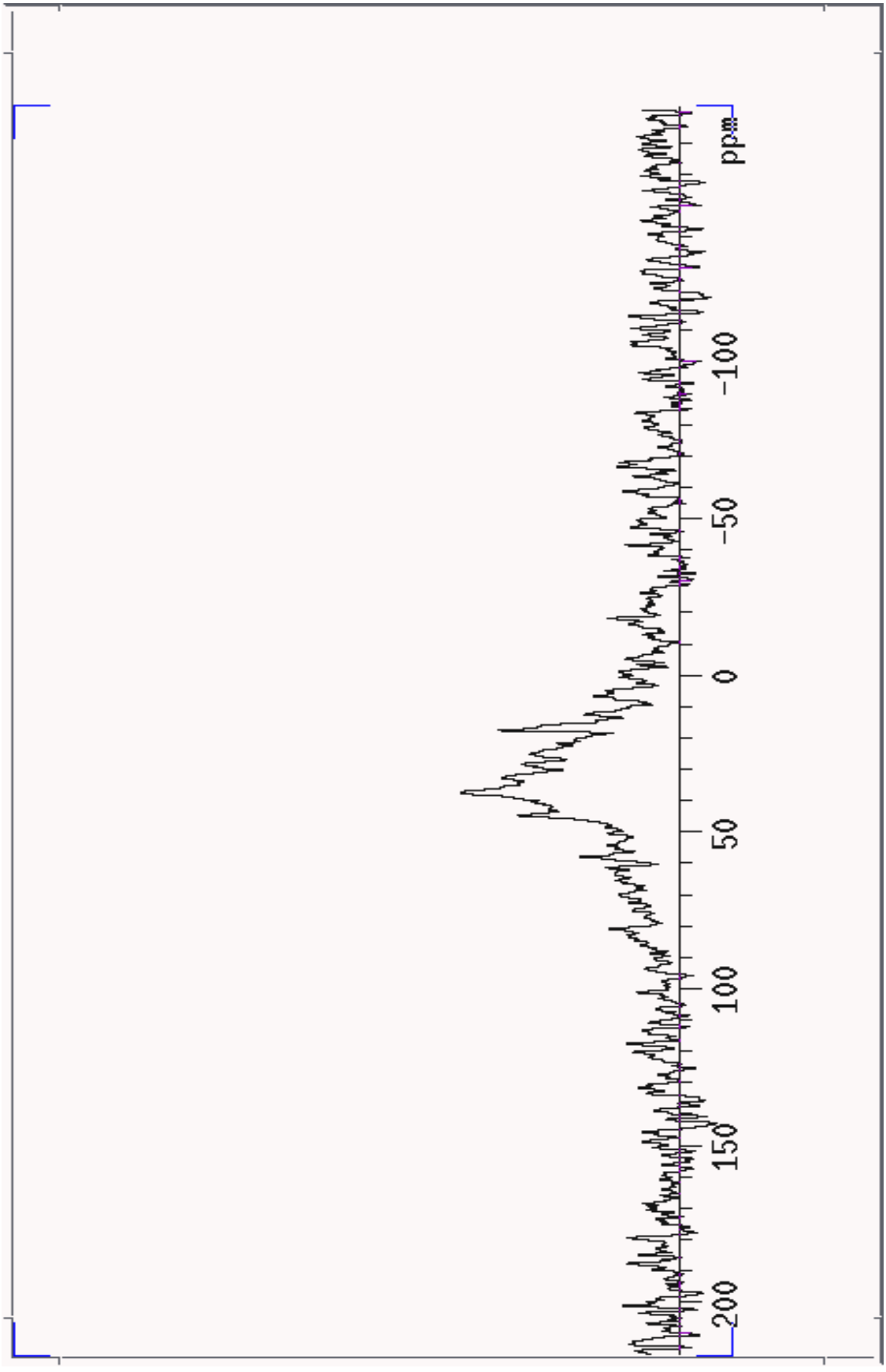

Figure 3.18 N^{15} NMR of CNF templated PPy deposited via 6 times cycling at 25 mV/s scan rate.

3. 2. 2. FTIR

The FTIR spectra of CNF templated PPy is slightly tilted inclining that the material is conducting.

- The major peaks are 2329 cm^{-1}, 2091 cm^{-1} and 1991 cm^{-1}.
- The first major peak is the indication of sp^3 hybridized C–H peak.
- The intense peak at 2091 cm^{-1} can be the conjugated C–C bonds, since the electron delocalization causes a downside shift.
- The third major peak is the stretching peak of aromatic, sp^2 hybridized C=C bonds
- The three peaks over 3000 cm-1 aromatic C–H peaks.

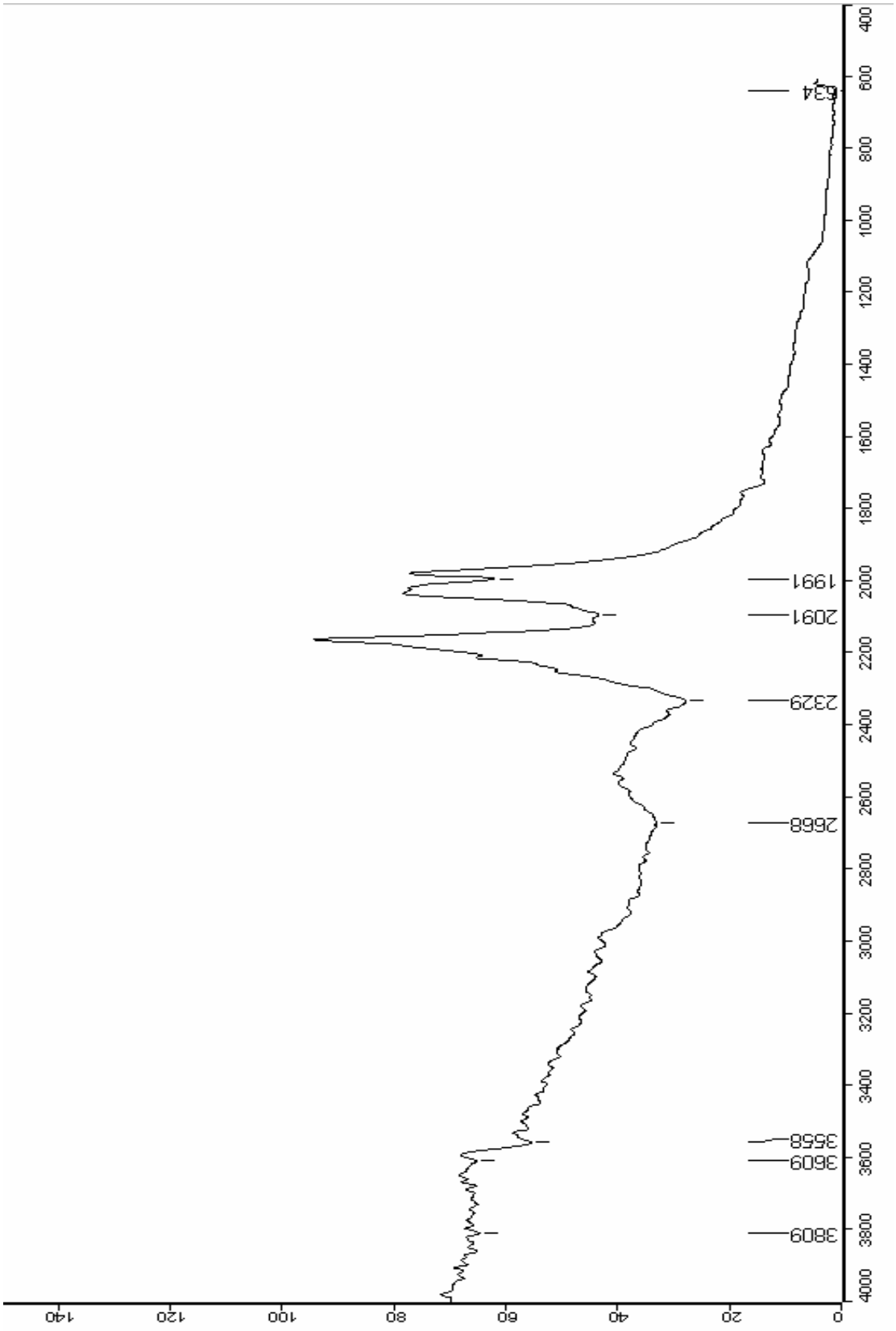

Figure 3.19 FTIR spectrum of CNF templated PPy deposited via 6 times cycling at 25 mV/s scan rate.

3. 2. 3. Voltammetry

3. 2. 3. a. Scan Rate Dependence

Mass transport basically depends on three main issues: convection, migration and diffusion. Convection can be controlled by not giving any disturbance to cell during the ongoing reaction. Also migration can be eliminated, or more realistically reduced to its minimum by increasing the amount of the electrolyte. For the latter, since the transfer rate of an electron is much higher than the diffusion rate of it, we simply should always have the same amount of electrons in the diffusion layer of the electrode in order not to be dependent on diffusion. By observing the polymer growth at different scan rates, we can comment if the electrochemical reaction is effected by diffusion or not. Normally polymerization of pyrrole does not depend on scan rate. As seen in the Figure 3.14(a), current densities of the Polypyrrole shows a relativity by means of increase as the scan rate is increased, explaining as the polymer scanned more and more fast, we have more electron in the diffusion layer although the concentration is always kept constant, proving the cell reaction is diffusion independent. However, this is not the case for CNF templated PPy samples as seen in F3.14 (b). This situation may arise from the fact that the infinitely small distance from the electrode is not smooth, therefore the e^- concentration around the surface may differ with different scan rates. Although, it is obvious that the highest peak current is obtained with 25 mV/s scan rate.

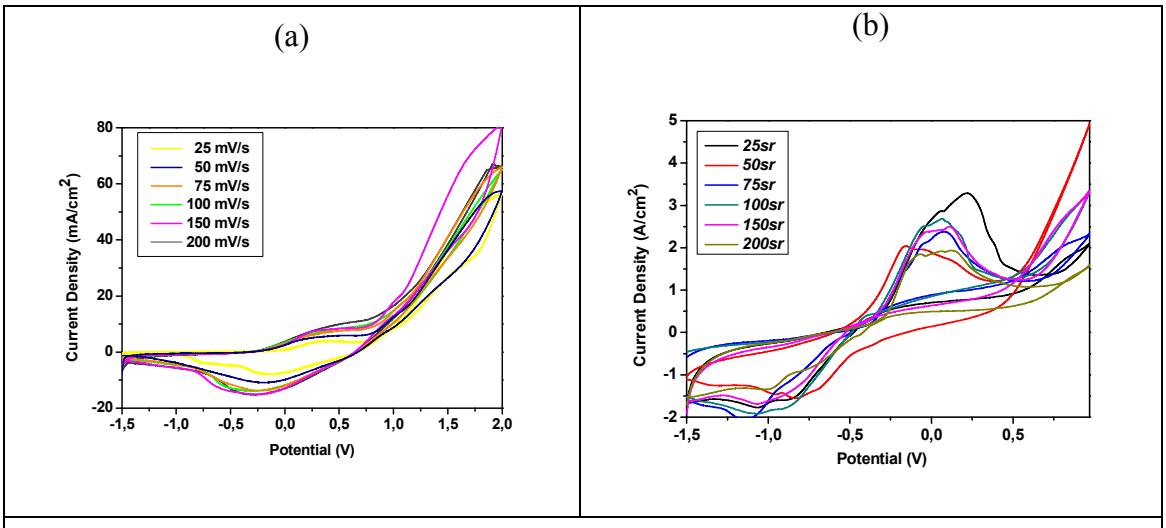

Figure 3.20 Scan rate dependence voltammograms of PPy (a) on ITO (b) on CNF

3. 2. 3. b. Specific Capacitance Value Calculation

Specific capacitance values for each sample is calculated from the area under the last CV curve.

CHAPTER 4

CONCLUSION

In this study, pyrrole monomer is polymerized on carbon nanofibers via electropolymerization. Its optimization has done by means of deposition amount and deposition speed.

- A new technique has been developed to have chemically bonded CNF-PPy active material unlike the composites used for supercapacitor technology nowadays.

- This new technique can have many derivations with different types of CNF's and CP's, to obtain a better active material with higher surface area and higher specific capacitance.

- Optimization has proven that the high deposition amounts result in blocks of polymers, which can be overcame by optimizing the amount of polymerization.

- The optimum deposition amount is found out to be 6 times cycling at 25 mV/s which is a relatively slow scan rate. The sample surface area was founded as 600 m^2/g from BET calculations.

REFERENCES

[1] G. Inzelt, M. Pineri, J.W. Schultze and M.A. Vorotyntsev, *Electrochimica Acta*, 45, **2000,** 2403.

[2] H. A. Pohl, *Chem Eng*., 68 (22), 105, **1961**, 105.

[3] H. A. Pohl and E. H. Engelhardt, *J. Phys. Chem*, 66, **1962**, 2085.

[4] R.L. Greene, G.B. Street, L.J. Suter, *Phys. Rev. Lett.*, 34, **1975**, 577.

[5] G. MacDiarmid, *J. Am. Chem. Soc.,* 98, **1976**, 3884.

[6] M.. Akta, *J. Chem. Soc. Chem. Commun.,* 1977, 846.

[7] D. Kumar, R. C. Sharma, *Eur. Polym. J*, 34 (8), **1998**, 1053.

[8] T. Ito, H. Shirakawa and S. Ikeda, *J. Polym. Sci., Part A: Polym. Chem.*, 12(1), **1974**, 11.

[9] J. J. Grodzinski, *Polym. Adv. Technol.*, *13*, **2002**, 615.

[10] C. K. Chiang, Y. W. Park, A. J. Heeger, H. Shirakawa, E. J. Louis and A. G. MacDiarmid, *J. Chem. Phys.,* 69, **1978**, 5098.

[11] P. J. Nigrey, A. G. MacDiarmid and A. J. Heeger, *J. Chem. Soc., Chem, Commun.*, **1979**, 594.

[12] D. Jr. MacInnes, M. A. Druy, P. J. Nigrey, D. P. Nairns, A. G. MacDiarmid and A. J. Heeger, *J. Chem. Soc., Chem, Commun.,* **1981**, 317.

[13] H. Shirakawai, E.J. Louis, A.G. MacDiarmid, C.K. Chiang and A.J. Heeger, *J. Chem. Soc. Chem. Commun.*, **1977**, 578.

[14] K.K. Kanazawa, A.F. Diaz, R. H. Geiss, W.D. Gil, J. F. Kwak, J.A. Logan, J.F. Rabolt, and G. B. Street, J. Chem. Soc. Commun., **1979**, 854.

[15] J. Heinze, *Syn. Met*., 41-43, **1991**, 2805.

[16] J.A. Chilton and M.T. Goosey, Special Polymers for Elcetronics and Optoelectronics, UK, Chapman and Hall, 1995.

[17] H. Shirakawa and S. Ikeda, *Polym. J*., 2, **1971**, 231.

[18] L. Alcacer, Condcuting polymers Special Applications, Holland, Riedel, **1987**.

[19] J. L. Bredas, R. R. Chance and R. Silbey, *Phys. Rev.,* Part B., B26 (10), **1982**, 5843.

[20] S. Dhawan, K. Kumar, M.K. Ram, S. Chandra and D.C. Trievedi, *Sens. Actuat. B*, 40, **1997**, 99.

[21] E. Aslan, *Characterızatıon Of Conductıng Polymers Of Ester Lınkage Contaınıng Thıophene Derıvatıves Vıa Mass Spectroscopy*, MSc. Thesis, Middle East Technical University, **2004**.

[22] J. Roncali, F, Garnier, M. Lemaire and R. Garreau, *Synth. Met*., 15, **1986**, 323.

[23] K. Doblhofer and K. Rajeshwar, edited by R. L. Elsenbaumer, R. J. Reynolds and T. A.Skotheim, Handbook of the Conducting Polymers, Vol 1, Marcel Dekker Inc., **1992**, USA

[24] S. Varis, M. Ak, C. Tanyeli, I. M. Akhmedov. and L. Toppare, *European Polymer Journal*, 42 (10), **2006**, 2352.

[25] S. Varis, M. Ak, C. Tanyeli, I. M. Akhmedov and L. Toppare, *State Sciences*, 8 (12), **2006**, 1477.

[26] S. Tarkuc, E. Şahmethoğlu., C. Tanyeli, I. M. Akhmedov and L. Toppare, *Sensors And Actuators B-Chemical*, 121 (2), **2007**, 622.

[27] B. Yiğitsoy, S. Varis, C. Tanyeli, I. M. Akhmedov and L. Toppare, *Thin Solid Films*, 515 (7-8), **2007**, 3898.

[28] A. Arslan, O. Turkarslan, C. Tanyeli, I. M. Akhmedov and L. Toppare, *Materials Chemistry And Physics*, 104 (2-3), **2007**, 410.

[29] E. M. Genies, G. Bidan and A. F. Diaz, *J. Electroanal. Chem.,* 149, **1983**, 101.

[30] R. J. Waltman and J. Bargon, *Tetrahedron,* 40, **1984**, 3963.

[31] R. Bittehn, G. Ely, F. Woeffler, H. Münstedt, H. Naarman and D. Naegele, *Makromol. Chem., Macromol Symp.,* 8, **1987**, 51.

[32] M. Satoh, S. Tanaka, K. Kaeriyama, J. Chem. Soc. Chem. Commun.,**1986**, 873.

[33] T. Nakajima and T. Kawagoe, *Synth. Met*., 28, **1989**, C629.

[34] O. Inganas and I. Lundstrom, *Synth. Met*., 21, **1987**, 17.

[35] G. Sonmez and F. Wudl, *Journal Of Materials Chemistry*, 15(1), **2005**, 20**.**

[36] G. Sonmez, *Chemical Communications*, 2005, 5251**.**

[37] G. Sonmez and H. B. Sonmez, HB, *Journal Of Materials Chemistry*, 16(25) **, 2006,** 2473.

[38] A. Durmus, G. E. Gunbas and L. Toppare, *Chemistry of Materials*, 19(25), **2007**, 6247.

[39] P.J. Negrey, C. Machine, D.P. Nainns, A.G. MacDiarmid and A.J.Heeger, *J. Electrochem Soc.*, 128, **1981**, 1651.

[40] J. H. Kaufman, T.C. Chun, A. J. Heeger and F. Wudl, *J. Electrochem. Soc*., 131, **1984**, 2092.

[41] Kitani, M. Kaya and K. Sasaki, *J. Electrochem. Soc.,* 133, **1986**, 1069.

[42] S. Iijima, Helical Microtubules of graphitic carbon, Nature 354, **1991**, 56.

[43] M. Terrones, *International Materials Reviews*, 49, **2004**, 325.

[44] J. Liu, S. S. Fan, and H. J. Dai, *MRS Bulletin*, 29, **2004**, 244.

[45] H. J. Dai, *Accounts of Chemical Research*, 35, **2002**, 1035.

[46] R. C. Haddon and S. -Y. Chow, *Pure Appl. Chem*, 71, **1999**, 289.

[47] N. Wang, G. D. Li and Z. K. Tang, *Chem. Phys. Lett.*, 339, **2001**, 47.

[48] G. Eres, A. A. Puretzky, D. B. Geohegan and H. Cui, *Appl. Phys. Lett.*, 84, **2004**, 1759.

[49] A. Thess, R. Lee, P. Nikolaev, H. J. Dai, P. Petit, J. Robert, C. H. Xu, Y. H. Lee, S. G. Kim, A. G. Rinzler, D. T. Colbert, G. E. Scuseria, D. Tomanek, J. E. Fischer and R. E. Smalley, *Science*, 273, **1996**, 483.

[50] S. Iijima, *Nature*, 354, **1991**, 56.

[51] H. Dai, A. G. Rinzler, P. Nikolaev, A. Thess, D. T. Colbert and R. E. Smalley, *Chemical Physics Letters*, 260, **1996**, 471.

[52] M. J. Height, J. B. Howard, J. W. Tester and J. V. B. Sande, *Carbon*, 42, **2004**, 2295.

[53] Michael J. O'Connell, *Carbon Nanotubes: Properties and Applications*, Taylor & Francis Group, London, **2006**.

[54] M. Inagaki, *New Carbons: Control of Structure and Functions*, Elsevier, Amsterdam, **2000**.

[55] R. C. Bansal, J. Donnet and F. Stoeckli, *Active Carbon*, Marcel Dekker, New York, **1988**.

[56] X. Py, A. Guillot and B. Cagnon, *Carbon*, 41, **2003**, 1533.

[57] H. P. Boehm, *Carbon*, 32, **1994**, 759.

[58] M. A. Montes-Moran, D. Suarez, J. A. Menéndez, E. Fuente, L. R. Radovic, F. S. Cannon and V. Strelko, *Carbon*, 42, **2004**, 1219.

[59] Y. Gogotsi, *Carbon Nanomaterials*, Taylor & Francis Group, Pennsylvania, **2006**.

[60] T. Yoshitake, Y. Shimakawa, S. Kuroshima, H. Kimure, T. Ichihashi, Y. Kubo, D. Kasuya, K. Takahashi, F. Kokai, M. Yudasaka, and S. Iijima, *Physica B*, 323, **2002**, 124.

[61] B. E. Conway, *Electrochemical Supercapacitors – Scientific Fundamentals and Technological Applications*, Kluwer Academic/Plenum, New York, **1999**.

[62] E. Frackowiak and F. Beguin, *Electrochem. Commun.*, 6, **2004**, 566.

[63] R. Kötz and M. Carlen, *Electrochim. Acta.*, 45, **2000**, 2483.

[64] A. Burke, *J. Power Sources*, 91, **2000**, 37.

[65] M. Mastragostino, F. Soavi and C. Arbizzani,, *Advances in lithium-ion Batteries*, Kluwer Academic/Plenum Publishers, Dordrecht, **2002**.

[66] M. Mastragostino, C. Arbizzani and F. Soavi, *Solid State Ionics*, 148, **2002**, 493.

[67] V. Khomenko, E. Frakowiak and F. Béguin, *Electrochimica Acta*, 50, **2005**, 2499.

[68] S. Brunauer, P. H. Emmett and E. Teller, *J. Am. Chem. Soc.*, 60, **1938**, 309.

[69] M. Balci, *Basic ^{1}H- and ^{13}C- NMR Spectroscopy*, Middle East Technical University, Ankara, Turkey, **2005**.

* Starred chapter only describes how the carbon nanofibers were synthesized originally by Ahu Gümrah Dumanlı, a PhD student from Sabancı University, it is not unique to this work.